UNIVERSITY

CAMPUS BIO-MEDICO OF ROME

PhD IN BIOENGINEERING AND BIOSCIENCES

Curriculum *(Biomedical Engineering)*

XXX CICLE (2014-2015)

"*Design and validation of sampling devices for ocular surface and fluids*"

Bijorn Omar Balzamino

Coordinator:
Prof. Giulio Iannello

Supervisor:
Prof: Loredana Zollo

Co-supervisor:
Dr.: Alessandra Micera

08 May 2018

CONTENTS

FOREWORD

It's far more important to know what person

the disease has than what disease the person has.

Hippocrates (c. 460 BC – c. 370 BC)

Since the complete sequencing of the Human Genome in April 2003, there has been an increasing attention on genomics in medicine, combined with efforts to incorporate genomic information into healthcare practice. (**Academy of Medical Sciences. May 2015**) It was not until the 19th century, however, that developments in chemistry, histochemistry and microscopy allowed scientists to begin to understand the underlying causes of disease. The treatment to patients dates back at least to the time of Hippocrates (**Egnew and Thomas, 2009**), but the term has risen in usage in recent years given the growth of new diagnostic and informatics approaches that provide understanding of the molecular basis of disease, particularly genomics. (**Morgan TH, 1932**). Midway through the century, observations of individual differences in response to drugs gave rise to a body of research focused on identifying key enzymes that play a role in variation in drug metabolism and response and that served as the foundation for pharmacogenetics (**Church D, 2014**). Human genome sequencing set in motion the transformation of personalized medicine from an idea to a practice. (**Offit K, 2011; Wilson B, 2015**). The aim of personalized medicine is to simplify clinical decision by differentiating those patients who benefit from a given treatment from those who will incur in side effects without gaining benefit (**Pavelic K).**

ACRONYMS

FDA	**Food and Drugs Administration**
DNA	**DeoxyriboNucleic Acid**
RNA	**RiboNucleic Acid**
MUC5AC	**Mucin 5AC**
IVDS	***in vitro* Diagnostic Devices**
MMP-9	**MetalloProteinase 9**
TRIS	**Tris(hydroxymethyl)aminomethane**
NACL	**Sodium Chloride**
CK	**Cytokeratin**
RCS	**Royal College Surgeon Rats**
PBS	**Phosphate-Buffered Saline**
PBS-TW	**PBS and 0.05% of Tween-20**
BSA	**Bovine Serum Albumin**
HRP	**Horse Radish Peroxidase**
ECL	**Enhanced Chemiluminescence**
TLR	**Toll Like Receptor**

ELISA	**Enzyme-Linked Immunosorbent Assay**
WB	**Western Blot**
ANOVA	**Analysis Of Variance**
NGF	**Nerve Growth Factor**
trkA^{NGFR}	**Tyrosine Kinase Receptor A**
p75^{NTR}	**panNeuroTrophine Receptor 75**
RBCs	**Rod Bipolar Cells**
RGCs	**Retinal Ganglion Cells**
INL	**Inner Nuclear Layer**
GCL	**Ganglion Cell Layer**
IFT	**Institute of Translational Pharmacology**
IMM	**Institute of Microelectronics and Microsystems**
ISM	**Institute of Matter Structure**
CNR	**National Research Council**
SAM	**Self-Assembled Monolayer**
AU	**Gold**
IL6	**Interleukin 6**
XPS	**X-ray Photoelectron Spectroscopy**

EIS	**Electrochemical Impedance Spectroscopy**
ASL	**Local Health Authority**

FIGURE LEGEND

INTRODUCTION

Personalized medicine is a growing field in which physicians and biologists use diagnostic tests to identify specific biological markers, which will determine medical treatments and procedures for each patient. Merging the researcher information with medical records, allows clinicians to develop targeted treatment and prevention plans (**Offit K, 2011; Wilson B, 2015**). Various scientific publications describe extensively the personalized medicine, health information management, biomarker discovery and targeted therapies (**Zhang L, 2015**). The market of molecular diagnostics devices is growing fast, nearly 4000 new diagnostic tests have been introduced only in 2015 (**Pritchard DE, 2017**). Equal for the molecular therapeutics market, nearly 28% of all the medicines the United States Food and Drugs Administration (FDA) approved in 2015 were personalized medicines (**https://www.fda.gov/Drugs/DevelopApprovalProcess**), and a recent study sponsored by the Personalized Medicine Coalition (PMC) demonstrated that 42% of all medicines and 73% of cancer medicines in development are potential personalized medicines (**Pritchard DE, 2017**). To realize a personalized approach new technology that endorses a person's biology, like DNA, RNA, or protein, to confirm a possible disease is required (**Vogenberg FR, 2010**).

In human medicine, and in particular in Ophthalmology, suitable cellular markers can be used to recognize corneal and conjunctival pathologies; their use is very useful for the diagnosis of ocular diseases. These markers provide great help both from a diagnostic point of view and from a therapeutic point of view. This type of investigation would in fact determine benefits from the etiopathogenetic point of view, clinical, diagnostic and prognostic for the pathology in consideration.

Hence, the main aim of my Ph.D. was to simplify the discovery of specific eye disorder biomarkers, through the development of new sampling and testing

devices, that allow the identification of a specific biomarker, correlated to a specific pathology, in office.

Therefore, my functional intent for the present thesis as shown in **scheme 1** was to undergo the simplification of biomarker discovery, through the design and development of three different devices:

- First a new sampling device, that incorporates a nitrocellulose membrane, that permits a fast and reliable imprinting and analysis of the ocular surface, as compared to other old sampling techniques, referring to biochemical and molecular analyses in order to identify and have an overview of the enormous field of the Biomarkers.
- Second a solubilizing device, that attends to solubilize the proteins and nucleic acids contained in biological fluids, or from the nitrocellulose membrane of the new sampling device, obtaining therefore samples immediately available for analysis.
- Third a biosensor, to facilitate the research of biomarkers of interest, I have participated in the development of a biosensor, for an already patented device, that will complete it, giving a quantifiable biomarker response, in collaboration with the ISM, IMM IFT institutes of the CNR of Tor Vergata.

This last device will give an immediate and quantitative response of a biomarker, solubilized in the second device in which both the biological fluids and the nitrocellulose membrane of the first device can be inserted, contributing to pursuing, therefore, the same goal, or the easiest identification of one or more specific pathology markers.

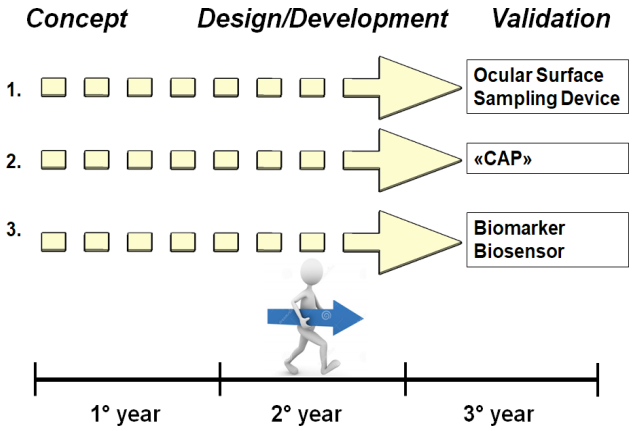

Scheme 1

From the concept to the prototype production and experimental validation.

The thesis is therefore structured to highlight an important issue in a current scenario of biosamples and biomarkers sampling devices

- Chapter 1 is an introduction to the world of the eye, a short overview of the anatomy of the eye and its pathologies, and a state of art about sampling devices.
- Chapter 2 will describe the proposed development and validation of the new ocular surface sampling device, enabling the physician to advise a personalized verdict, after analyzing the state of the ocular surface.
- Chapter 3 will introduce a second device, a container of extraction solutions useful for the solubilization of samples from different biological materials. This new device will reduce the waiting time and extraction of proteins or nucleic acids, obtaining immediately samples already analyzable.
- Chapter 4 describes the development and validation of a biosensor that rearranges an old patented device for the detection of different biomarkers in biological fluids. To standardize the lectures with this device, an additional approach has been undertaken, and the incorporation of a biosensor actually in commerce evolved this old device.

- Chapter 5 will discuss the results obtained and will give an overall conclusion on the future perspectives.
- The thesis will end with a list of Publications and with a short Bibliography

CHAPTER 1

The World of the Eye

1.1 Anatomy of the eye

The eye is the organ responsible for vision, formed by the bulb, eyebrows and ocular anecdotes, the muscles that move the bulb, the eyelids that protect it, and the tears that keeps damps the exposed parts to the air.
The ocular bulb consists of three tunicae: an external fibrous tunica, an intermediate vascular tunica and an internal nervous tunica. In the eyeball we recognize three cavities: the front chamber and the rear chamber, communicating with each other, containing a liquid substance called water humor and more deeply, the vitreous cavity, which contains vitreous mood.
The eye is the peripheral organ of the visual system, where the outer surface is an incomplete and opaque sphere constituted by the sclera for the 93%, which is interrupted on the front-end, by the cornea, a second smaller transparent spherical portion, about 7% of the total surface and of different curvature.

The retina, essential component of the eye, is the primary purpose for vision. All other structures of the eye are secondary and act to focus images on the retina, to regulate the amount of light, to provide nutrition, protection or motion (**McCaa CS, 1982**).

The cornea is unique because of its transparency. Corneal transparency is dependent on a special arrangement of cells and collagenous fibrils in an acid mucopolysaccharide environment and to an absence of blood vessels (**McCaa CS, 1982**).

The ocular globe has an irregular diameter: the transverse diameter measures 23.7 mm, the vertical diameter is 24.2 mm, the antero-back diameter is about 24.8 mm; Its volume is about 6000-7000 mm^3. The weight of the eye is around 7-8 grams

and it consistency is due to the fluid pressure (15 mm/Hg) contained in the ocular globe cavity (**Bekerman I et al., 2014**).

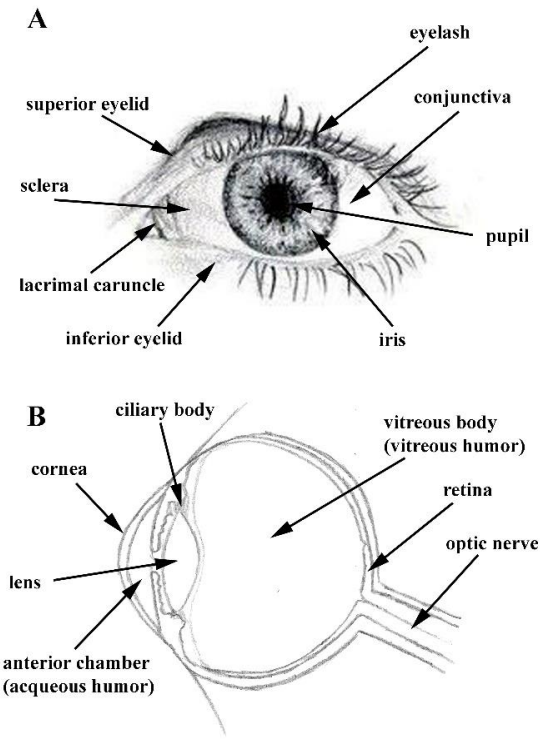

Figure 1
Front vision of the eye (**A**) and Horizontal section of the eye (**B**)

1.1.1 Conjunctival Disorders

The conjunctiva is a transparent mucous membrane on the sclera, that lays in front of the posterior face of the eyelids (tarsal conjunctiva) and the outer surface of the sclera just before the cornea (bulbous conjunctiva). (**Figure 1B**).
The Tarsal conjunctiva appears generally smooth and the conjunctival epithelium appears to be non-keratinized and stratified with calcium-forming cells producing mucin, namely the mucin 5AC (Muc5Ac), an important component of the tear film and columnar cells that usually have a microcircle layer and accumulate lymphocytes.

The bulbous conjunctiva is instead composed by a squamous epithelium stratified in continuity with the corneal epithelium (**Marko CK et al., 2014**).

Physiologically the conjunctiva performs the following functions: elasticity, defensive ability, protective capability and ability to spread (**Dartt DA and Masli S, 2014**).

Diagnosis can be carried out using numerous tests, some of which are used to diagnose the quality of the tear film (such as tear film disruption), while others measure the quantitative lacrimation deficits (such as Schirmer tests) (**Lin H et al., 2014**).

Laboratory tests are generally not necessary, but may be useful in some cases. (**Irkeç M and Bozkurt B, 2003**).

1.1.2 Corneal disorders

Corneal lesions and diseases such as: guttural cornea, corneal dystrophy, corneal ulcer, keratoconus, corneal abrasion can lead to loss of corneal transparency.

Granular corneal dystrophy is also known as Groenouw type I corneal dystrophy. It is a corneal disease characterized by the presence of small whitish opacities at the level of the axial front corneal stroma visible to the slit lamp. Diagnosis remains clinical and instrumental. There is currently no diagnostic test. Histology shows amorphous hyaline deposits shining in bright red with the Masson trichrome staining (**Seitz B and Lisch W, 2011**).

Keratitis is a cornea inflammation, that manifests itself with pain and vasodilation on the conjunctival membrane (the symptoms are like those of conjunctivitis). Keratitis can be superficial, if located at epithelium level and frontal layers of the cornea, or deep, if inflammation also involves the endothelium (**Lambiase A et al., 2008; Patel DS et al., 2017**).

A corneal ulcer is a serious corneal injury, usually caused by an inflammatory process or an infection. Corneal ulcers appear as small sores on the cornea. The symptoms include progressive redness, foreign body sensation, pain, photophobia

and tearing. Diagnosis is carried out with the slit lamp, fluorescein coloring and microbiological examinations (**Aloe L et al., 2015; Micera et al., 2007**).

The keratoconus, is a degenerative cornea disabling disease, it usually manifests itself with a gradual loss of sight, astigmatism and myopia. The cause of the disease is still unclear, but there seems to be a genetic predisposition (found in 10-15% of cases). It can affect one or both eyes (**Lambiase A et al., 2005**).

1.1.3 Retinal disorders

Retinopathy is a generic term with reference to a large group of pathologies affecting the retina (the inner membrane of the eyepiece bulb). Below is a brief overview of some of them.

Retinal detachment occurs when the retina detaches from the underlying tissue, known as the choroid. If detachment involves the most central area of the retina, macula lutea, vision loss is particularly severe and the chances of recovering the sight diminish considerably (**Ripandelli G et al., 2015**).

Age-related macular degeneration is a progressive ocular pathology that causes a non-reversible deficit of central visual function. The causes of senile maculopathy are not fully known; it is believed that there is a combination of environmental and genetic factors that pose the greatest risk to contracting the disease (**Cacciamani A et al., 2016**).

The Retinitis pigmentosa is an improper terminology with which we refer to a group of hereditary pathologies different from each other that are associated with a degenerative evolutionary process that results in a decrease in the efficiency of retinal receptors, cones and rods (**Rocco ML and Balzamino BO, et al., 2015; Rocco ML and Balzamino BO et al., 2017**).

The Retinoblastoma is a malignant tumor affecting the retina and commonly developed in the first five years of life. Etiology is unknown; all the various forms of the neoplasm are triggered by an alteration of the RB1 onco-suppressor gene (**Journée-de Korver HG et al., 2005**).

Diabetic Retinopathy, among the various retinopathies, it is perhaps one of the most commonly found; is in fact the most common ocular complication of diabetes mellitus.

At its initial stages, the disease is asymptomatic; among the most common symptoms we find blurred vision, loss of visual acuity, perception of dark areas in the visual field, myopia, and difficulty in correctly perceiving colors. In the worst cases you arrive to blindness (**Vujosevic S et al., 2015; 2016**).

The Glaucoma is a subtle disease that affects the eye, slowly destroying the sight. About two million people suffer in Italy. Fortunately, an early diagnosis, associated with the right therapies, is able to block the evolution to the minimum damage for the sight. When, the pressure inside the bulb exceeds the normal 14-16 mmHg value it can damage the optic nerve, a direct connection to the brain (**Micera A et al., 2016**).

1.2 State of Art on the Sampling devices

Medical Devices

"Device" is defined as "an instrument, apparatus, implement, machine, contrivance, implant, in vitro reagent, or other similar or related article, including any component, part, or accessory, which is [among other things]… intended for use in the diagnosis of disease or other conditions, or in the cure, mitigation, treatment, or prevention of disease, in man or other animals … and which does not achieve its primary intended purposes through chemical action within or on the body of man or other animals and which is not dependent upon being metabolized for the achievement of its primary intended purposes." Section 201(h) of the Federal Food, Drug, and Cosmetic Act (FD&C Act), 21 U.S.C. § 321(h).

In Vitro Diagnostic Device

A medical device is an in vitro diagnostic medical device (IVD) is defined by the European Union specific directive as any medical device which is a reagent, reagent product, calibrator, control material, kit, instrument, apparatus, equipment, or system, whether used alone or in combination, intended by the manufacturer to be used in vitro for the examination of specimens. It must be intended by the manufacturer to be used in vitro for the examination of specimens derived from the human body, solely or principally for the purpose of giving information about a physiological or pathological state, a congenital abnormality or to determine

safety and compatibility with a potential recipient, or to monitor therapeutic measures. [41 FR 6903, Feb. 13, 1976, as amended at 45 FR 7484, Feb. 1, 1980]

Diagnostic tests are planned to measure (in case of *in vitro* diagnostics), or evaluate, an indicator (biomarker) of a normal biological process, pathogenic process, or in response to a therapeutic plan (**Biomarkers Definitions Working Group, 2001**). In personalized medicine, where the diagnostic test is a biomarker-based assay, the clinical power of the test refers to a percentage of validity of the test (**Lai TL, 2012**). Many of the diagnostic tests used in personalized medicine are *in vitro* diagnostic devices (IVDs), also called clinical laboratory tests, which test body substances from patients for alterations in levels of biomarkers (e.g., proteins) and the presence/absence of genetic susceptibility biomarkers (**Cohen JP, 2014**). Moreover, the complexity of these tests is ever evolving, as single marker tests have given way to tests that measure multiple markers simultaneously, such as complex gene panels (**Gulley ML, 2010**). In **figure 2** is shown a comparison between IVD's and LDT's from authorization to distribution. Another challenge associated with ensuring the safety and reliability of IVDs is that they may be marketed in one of two ways: as IVD kits or as laboratory developed tests (LDTs) (**Burd EM, 2010; Marton MJ and Weiner R, 2013**).

Requirements	IVDs	LDTs
Marketing Authorization	FDA/Section 520 FD&C Act	CMS/CLIA Standards
Time to Develop	Long (12-24 months)	Short (4-6 months)
Subject to Quality Systems • Design Controls • Manufacturing Controls • Complaint Handling	Yes	No
Establish Clinical Validation prior to marketing	Yes	No
FDA guidance for use as a companion diagnostic	Yes	No
Global Reach/Distribution	Yes	No

Figure 2
Comparison of IVDs & LDTs (Source: Biotechnology Entrepreneurship: Starting, Managing and Leading Biotech Companies).

Molecular Diagnostics. Blood, tissue, tears or other biological samples can be used in laboratory tests to identify the presence of specific molecular biomarkers. Molecular diagnostics can be used to assess the efficacy of a specific therapeutic agents, identify patients not suitable for a given treatment or dosage, determine optimal dosages for drugs, monitoring the progression of disease or examine clinical outcomes (**Alomar MJ, 2014, Balzamino B et al., 2015; Rocco ML et al., 2015,2016,2017; Aloe L et al., 2015,2016; Micera A et al., 2016**).

Currently in the clinic, sampling is often carried out after informed consent, by laboratory instruments adapted for the occurrence or through devices actually in commerce. Referring to my aim, the research of biomarkers can be pursued through the sampling of biological fluids, such as tears, saliva, etc., but also through an impression cytology of the ocular surface. The most important sampling devices in an ophthalmological clinic are reported below.

1.2.1 Impression cytology

Ocular cytology was used for the first time in 1954 by Larmande and Timsit for the diagnosis of a squamous neoplasm, but in England Egbert and his collaborators in 1977 used for the first time a cellulose membrane to analyze the presence of goblet cells, Mucin secreting calcium-forming cells, in patients with dry eye syndrome concluding therefore that from a light pressure of the ocular surface for a few seconds by pressing a cellulose membrane, they could obtain the imprint of the superficial cell layer (**Egbert PR et al., 1977**).

Impression cytology (IC) is an innovative and original diagnostic technique, which involves the application of a cellulose acetate filter on the ocular surface to sample (**Thiel M, 1997**). The modified method uses a cellulose acetate filter paper, which is cut into a 5-mm strip with a square end and a thin end. Studies show how the asymmetric, toe-shaped form facilitates the capture and transfer of the membrane to the desired area (**Tseng SCG, 1985**) as shown in **Figure 3.**

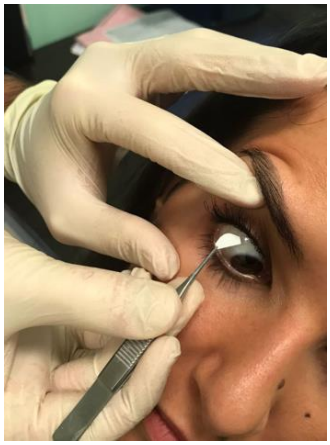

Figure 3
Modified sample collection method using a cellulose acetate filter paper and a tweezer.

With this type of investigation, the most superficial layers of the ocular epithelium are removed; usually it's about 1-3 layers that stick to the filter. The samples, thus obtained, can be subjected to histological, immunohistochemical or molecular analysis (**Nelson JD, 1988**).

Goblet cells, visible in fuchsia in **Figure 4AB,** in the discovery of impression cytology samples became one of the diagnostic features for dry eye, conjunctivitis, chemical damage and others (**Tsubota K, 1999**).

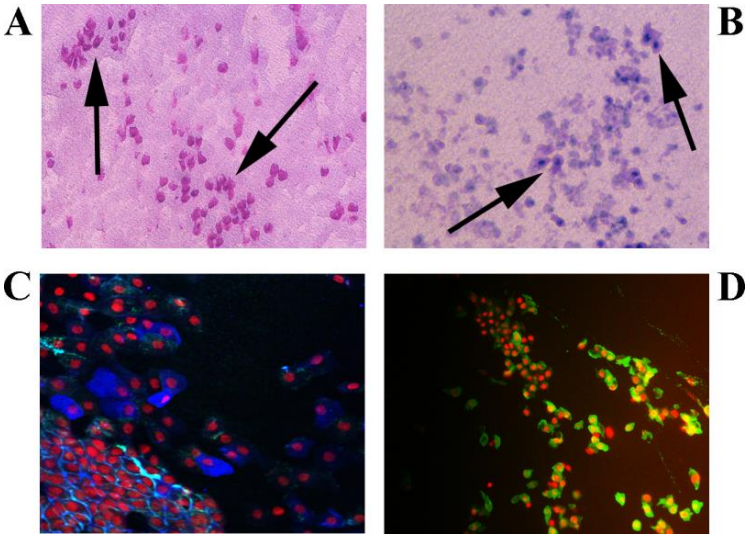

Figure 4
AB Examples of epithelial cells obtained from a cytology stained with specific colorants. Arrows indicate goblet cells, mucin secreting cells, involved in the homeostasis of the ocular surface. **CD** Impression cytology stained for cytokeratin's, specific markers for conjunctival cells in green, or corneal cells in blue. Nuclei are stained in red with Iodium Propide.

More recently, a new nitrocellulose Biopore membrane is used (The filters used are nitrocellulose filters, Millicell-CM Culture Plate Insert, 0.22 µm, Ø 12 mm, PICM 012 50, Millipore Corp., Bedford, MA, USA) as shown in **Figure 5**. Therefore, modified by different authors, this non-invasive technique has been rapidly adopted and used for histological studies on dry eyes, vitamin deficiencies, pemphigoid, ocular scarring, limb deficits, viral and bacterial infections, allergic disorders, conjunctival and malignant melanomas (**Singh R et al., 2005; Eördögh R et al., 2015**).

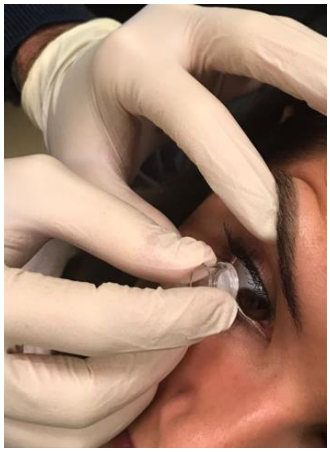

Figure 5
Millicell-CM Culture Plate Insert, 0.22 µm, Ø 12 mm, PICM 012 50, Millipore Corp., Bedford, MA, USA, used to obtain impression cytology's in outpatient clinics.

This sampling procedure preserves the morphology of the conjunctival and/or corneal epithelium and has the fundamental advantage of allowing unlimited use of cytodiagnostic techniques, from the simplest basic histological staining immunocytochemistry/immunofluorescence to DNA/RNA/proteins up to cytofluorometry (**Aronni S, 2006**).

Normal human ocular surface demonstrates a unique cytokeratin expression pattern containing characteristic cytokines, a non-keratinized, stratified (CK4 and CK12, green), simple (CK8 and CK19, blue) epithelium and glandular epithelium (CK7) (**Elder MJ, 1997**). Hence, to analyze the cytokines in the corneal, conjunctival and limbal epithelium it is possible to find out what deficits are present on the ocular surface (**Kurpakus MA et al., 1994; Sacchetti M et al., 2005**) (**Figure 4CD**).

Nowadays the main techniques used in outpatient clinic are the use of membranes positioned by the doctor on the conjunctiva and/or cornea of the patient, after anesthetizing the ocular surface with novesina and after leaving the membrane for 3 to 4 seconds, the membrane will be taken off and stored based on analysis to be performed on the sample; the use of Millicell CM 0.4µm PICM01250 membranes is one of the most used thanks to its flexibility, it is provided with a transparent plastic cylindrical support at its extremities; by a slight

pressure for a few seconds on the conjunctiva or cornea, the epithelial cells will be collected from the affected parts (**Figure 5**).

Samples are collected in Thin Prep (PreservCyt™ Solution) or fixed by Cytofix (Bioptica) and sent to the laboratory for subsequent analysis.

1.2.2 Micropipette or Microcapillary

A method for tear sampling is the use of micropipettes or microcapillaries, by which about two drops of saline are poured onto the eye, thus flushing the ocular surface and thereby diluting the sparse tear fluid. After a few blinks the ''eye flush saline'' is recollected and the content of tear proteins quantified (**Cacciamani A, 2016**). The average volume of tears collected without eye flush is on average 7µl ± 2µl and with the eye flush 57µl ± 4µl. The thickness of the tear film is 9µm ± 3µm and during blinking diminishes to 4µm ± 1µm. The production of tears is about 1,2ml/minute and diminishes with age. The pH range is 7,14-7,82 and the osmotic pressure in the morning is <320mOsm/Kg. The tear is composed by Electrolytes: Na+ (4,45 g/l), K+ (1,2 g/l), Cl (3,90 g/l); Proteins (60 types): for a total of 5g/l, the major ones are Albumin, Lactoferrin, Immunoglobulins (IgA; IgE; IgG; IgM), Lysozyme (30% of tears is composed by this kind of protein); free amino-acids, Glucose 0,65 (g/l) and exfoliated cells. (**Figure 6**)

Figure 6
Micropipette sampling methodology. In outpatient clinic micropipettes are still used to sample few µl of tears from patient with ocular surface disorders.

1.2.3 TearLab Osmolarity System™

The TearLab Osmolarity System is a device used to quantify human tears and its osmolarity in aid of the medical doctor in conjunction with other methods of clinical evaluation. The Reader has an LCD screen, a keypad, and an external AC power supply **Figure 7A**. Each Test Card is a single-use, nonsterile polycarbonate microchip containing (**A**) microfluidic channel to collect 50 nanoliters (nL) of tear fluid by passive capillary action, and (**B**) gold electrodes embedded in the polycarbonate microfluidic channel to enable on-board measurement of tear osmolarity. The Test Card does not contain chemicals or reagents (**Figure 7B**). TearLab test results are displayed on the LCD in mOsms/L, the range is linear from 275–400 mOsms/L; Normal tears have an osmolarity of Mean 309.9 mOsms/L ± 11.0 (288–331 mOsms/L; 90% CI 288–331), as shown in **Figure 7C**. a linear graph shows the different degrees of dry eye pathology, based on the osmolarity of tear fluid sampled.

The TearLab Osmolarity System is designed for stability, reliability, and safety, and it has been developed, manufactured, and marketed under a quality management system certified to ISO 13485 (2003).

The TearLab Osmolarity System complies with the following materials:

- WEEE Directive 2002/96/EC Waste Electrical and Electronic Equipment
- RoHS Directive 2002/95/EC Restriction of Hazardous Substances
- IEC 60601-1 Medical Electrical Equipment — General Requirements for Basic Safety and Essential Performance

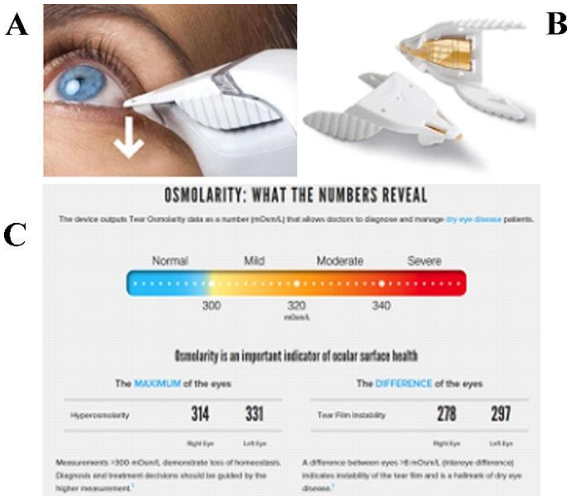

Figure 7
TearLab Osmolarity device. TearLab is a new medical device used in clinics to evaluate the osmolarity of the tear film, using a chip integrated in a sampling pen.

1.2.4 RPS Inflammadry™

RPS Inflammadry is a patented Direct Sampling Micro-Filtration (DSMF) and patent-pending Direct Multi-Planar Chromafiltography (DMC) technology. RPS tests provide rapid results with high sensitivity and specificity of MMP-9 protein in tear fluid samples taken from inner side of the eye, the palpebral conjunctiva. Product Name: Inflammadry (Catalog #: RPS-ID-20-U) detects elevated levels of MMP-9 ≥ 40 ng/mL in tears. If MMP9 is present in the tear sample, the protein is captured between a specific mouse monoclonal and goat polyclonal antibodies at concentrations ≥ 40 ng/mL. This antigen-antibody complex is captured by Neutravidin immobilized as the test line.

The buffer vial contains a buffered salt solution containing: 200 mM Tris, 10% Fish 81 (sea block), 0.8% Tergitol, 100 mM NaCl, 0.1% Sodium Azide, 0.0126% Gentamycin, pH 9.5 ± 0.05.

The unused device also has two faint orange lines in the result window. If the test is valid, a BLUE line will appear in the control zone as shown in **Figure 8**.

Figure 8
RPS Inflammadry is a novel sampling device, that provides rapid results of the presence of MMP9 in tears, for the diagnosis of dry eye.

1.2.5 EyePrim™

The EyePrim™ (American patent application US201 1/319789) is a medical device used to sample conjunctival cells from the eye developed by professor Baudouin (M.D., professor and chair of ophthalmology, Quinze-Vingts Hospital). EyePrim™ is a Class I (sterile) medical device according to the directive 93/42/CEE, CE 0499 (SNCH) and FDA exempted from Premarket Authorization Procedure according to the Code of Federal Regulation Title 21: 21CFR880.6025 (**Figure 9A**).

The membrane, at the end of the device shown in **Figure 9B**, has a half moon geometry and is composed of a polyether sulfone filter.

The membrane is placed at the bottom end and adapts to the shape of the device; consequently, the membrane must be detached from the device and placed in the liquid suitable for the type of analysis to be carried out. The device has a Scleral curvature and Limbal diameter that delimitates the cornea from the conjunctiva. The Volume of the membrane is 69 mm^2 and its composed by Polyether sulfone, optimized to obtain a best yield.

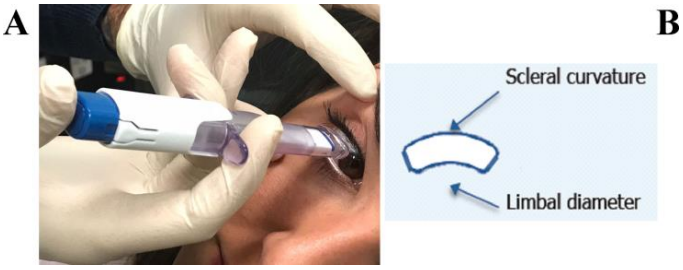

Figure 9

The EyePrim is an ocular surface sampling device, that permits to obtain by pressing the membrane on the conjunctiva, an imprinting of 3 to 4 layers of cells (**A**). Subsequently these cells, present on the membrane (**B**), may be analyzed in laboratory by microscopy after been treated for different laboratory techniques.

1.2.6 TEARPRIM™

TEARPRIM™ is a sterile medical device concept, designed to sample the tear. It is developed in close collaboration with Quinze-Vingts Hospital and ophthalmologists. This tear sampling device aims to replace the current sampling and the non-standardized techniques (capillary tube, Schirmer strip, etc.…). TEARPRIM™ allows the collection of a high quantity of tears in a minimally-invasive way.

TEARPRIM™ is a new Class IIa (sterile) medical device according to the directive 93/42/CEE, CE 0499 (SNCH). Poor data are available due to its poor use in outpatient clinic.

1.3 Conclusion

In conclusion, these devices may help the physician to obtain a sample analyzable, for the research of specific biomarkers, but not all are reliable or give a result of a specific biomarker. For example, the EyePrim makes an impression of the ocular surface, but the membrane used for it, does not give good quality results, as there are difficulties in the staining, of the cellular population, for the analysis of the ocular surface. TearLab Osmolarity, in contrary, quantifies human tears and its osmolarity, but does not search for a specific marker and moreover the cartridges

are very expensive. Finally, the RPS Inflammadry device, offers the detection of MMP9 for the diagnosis of dry eye. At present this marker has been abandoned as far as this pathology is concerned, since the correlation between the pathology and this protein has not been validated, since the expression of MMP9 in dry eye disease is likely a late-stage sign (**Schargus M et al., 2015**). Therefore, to pursue the finding of specific markers of eye disorders, my intent was to design and develop new sampling and testing devices capable to obtain a good sample for a good staining or for an immediate biomarker evaluation.

CHAPTER 2

A new ocular surface sampling device

Abstract

The aim of this study is to research different biomarkers for different eye pathologies, developing and evaluating a rapid sampling device for the ocular surface. The key idea of the present invention is to provide a device and a method for the sampling and analysis of the outer layers of the ocular surface, by impression cytology, solving the disadvantages of the devices of known art. The device is capable of significantly enhance the ocular surface sampling technique by reducing the time and discomfort for the patient, while increasing the level of effectiveness of the procedure. 10 sclero-corneal rings, obtained from donors of the Eye Bank of San Giovanni's Hospital, and 3 volunteers' participants were used for this test. The following sampling was performed by an ophthalmologist specialist and I carried out the processing in laboratory. The membranes were removed from the support and subjected to PAS staining (Periodic Acid Schiff/ Hotchkiss and Immunofluorescence for the Muc5AC and cytokeratin's. The evaluation was finally done by comparing the impression cytology obtained with the proposed sampling device and the MilliCell™ device. We concluded that this rapid new sampling device allowed successful detection of the ocular surface cells, in particular Goblet cells, with 95% sensitivity and specificity. We thus expect that this simple sampling device can be a suitable and affordable device for the routine clinical diagnosis, which will help in making precise diagnoses and help medical doctors.

2.1 Introduction

The introduction of new devices, mobile and wireless capability, better sensors, have led to technologies that allow a better monitoring and treatment even staying at home (**Ventola CL, 2014**). The concept of personalized medicine is not

new, what is new is that developments in science and technology open new paths for targeted therapeutics and tools (**Dingel MJ et al., 2015**).

In the field of research, medical, chemical and biological sciences, it is of great interest the activity aimed at the development of nanostructures for the analysis of molecules, using enzymatic assays currently employed in the laboratory. Therefore, the purpose of this Ph.D. thesis is to create a device that allows the sampling and analysis of the ocular surface, for the research of specific eye diseases biomarkers, with specific characteristics, for example It must significantly improve the current techniques of sampling, reducing the residence time of the membrane on the eye, and the discomfort for the patient, while increasing the level of effectiveness of the procedure. The use of this device must compensate for any involuntary or inaccurate tremor and movements of the operator, through the presence of a support for the stable positioning of the cytological sampling device. Specifically, I tried to create a device that allows rapid, simple, effective and non-invasive analysis of the epithelial cells of the ocular surface.

2.2 Design specifications

The constraints imposed by the design of the device and its essential features must comply with the technical specifications and allow the device to be fully adapted to the morphology of the ocular orbit, in this respect the anatomy of the eye has been specifically analyzed and the design developed with specific software's. Therefore, to meet these requirements, it was decided to develop a device consisting of two modules: pickup stick and periocular device B, the pickup stick has an ergonomic and elementary geometry, which emphasizes the simplicity of use, but at the same time is able to guide the operator in the execution of the procedure, thus extending the possibility of use even to non-expert operators. The pickup stick was designed for a dual use mode: in conjunction with a second element (also referred to as periocular device B) for assisted sampling, or in stand-alone mode for a manual sampling. The combination of the two devices, reduces the possibility of error of the operator by creating a standardized method and a guided procedure. Weighing less than 300 grams and having dimensions

compatible with those of the eye socket, facilitating positioning, reduces discomfort for the patient. Substantially the device has an elongated shape presenting at one of its ends an accommodation portion for a membrane suitable for sampling.

The periocular device B is a subsystem of the sampling device, it is composed by springs inserted in a linear guide allowing a passive regulation of the interaction forces on the eye, increasing the safety and considerably reducing the risk of damage. The joint use of the two elements of the device thus allows assisted sampling, with an increase in the level of accuracy, repeatability and safety. It rests on the bone part around the eyes, with the consequent advantage of unloading the forces on the bone without damaging the eye, compensating tremor and accuracy of the procedure. The periocular device B has a hole suitable for inserting the first pick up stick and allowing sampling at different points of the ocular surface simply by rotating the subsystem. The second element has therefore been designed to allow the insertion of the first element into the hollow portion inclined by 15 degrees.

Moreover, the kit contains a closing element, suitable to preserve the sample avoiding deterioration. The closing element has a specular geometry with respect to the pick-up device to allow a perfect housing of the lower portion of the stick inside it. The kit can thus furthermore also have suitable solutions for the biochemical, confocal or molecular for consequent analysis.

2.2.1 Analysis and dimensions of the eye curvature

As already mentioned in the preceding paragraphs, the cornea is the part of the eye, together with the conjunctiva, exposed to the outside and has a curvature smaller than the sclera, so protrudes forward.
The thickness of the cornea is variable, maximum at the sclero-corneal rim, where it arrives to measure about 0.65mm, minimum toward the center where the maximum protrusion is about 0.52mm. The curvature radius on the front surface is about 7.2mm, while on the back of about 6.8mm as shown in **Figure 10**.

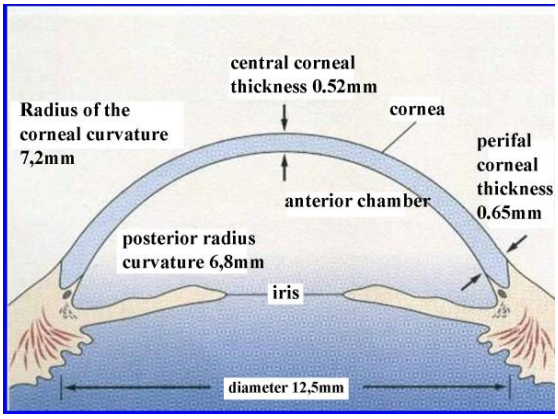

Figure 10
Analysis of the dimensions and the curving of the eye.

2.2.2 Force Analysis Studies

The force exerted by the operator during the cytological withdrawal might be a problem as if excessive force is applied, the risk is to damage the ocular epithelium while, if insufficient force is applied, an invalid sampling is performed obtaining a cell population that is insufficient for cytological analysis.

In this regard, a study of the force generally imprinted by the operator has been carried out, analyzing and measuring such forces by using the JR3 Multi-Axis Force Torque Sensor System (**Figure 11**).

The Sensor System is a force sensor that can define a load by measuring the forces on three orthogonal axes. The body of the sensor has six degrees of freedom and the output is in the form of a high speed synchronous serial data stream.
Each JR3 sensor is individually calibrated with loads on each axis. The calibration data is used to generate a calibration and a decoupling matrix, used to convert the output voltages. The calibration matrix is provided on the sensor's technical specifications.

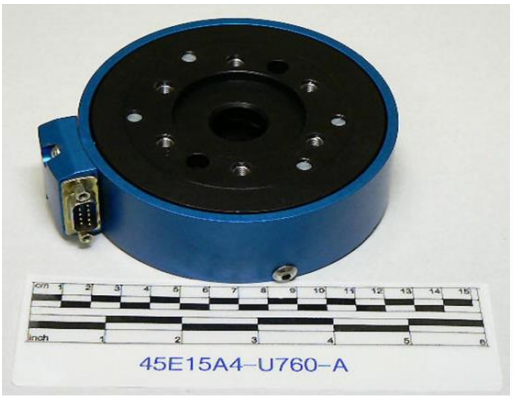

Sensor Model: / Mechanical Load Rating:	20E12A4 40N	20E12A4 100N	20E12S4 120N	20E12S4 300N
Diameter (mm)	51	51	51	51
Thickness (mm)	31.8	31.8	31.8	31.8
Material	AL 2024	AL 2024	SS 15-5PH	SS 15-5PH
Weight (g)	135	135	290	290
Nominal Accuracy, all axes (% measuring range)	±0,25	±0,25	±0,25	±0,25
Operating Temp. Range, non-condensing (°C)	-40 to +65	-40 to +65	-40 to +65	-40 to +65
F_x, F_y				
Standard Measurement Range (N)	±40	±100	±120	±300
Digital Resolution (N)	0,0050	0,013	0,015	0,038
Stiffness (N/m)	3,2e6	6,8e6	8,3e6	18e6
Single-axis Overload (N)	400	930	1050	2450
Multi-axis Overload Coefficient, a (N)	400	1030	1050	2700
Multi-axis Overload Coefficient, b (N)	490	930	1300	2450
F_z				
Standard Measurement Range (N)	±80	±200	±240	±600
Digital Resolution (N)	0,010	0,025	0,030	0,075
Stiffness (N/m)	35e6	68e6	91e6	180e6
Single-axis Overload (N)	1350	3100	3550	8150
Multi-axis Overload Coefficient, c (N)	1350	3100	3550	8150
M_x, M_y				
Standard Measurement Range (Nm)	±2,0	±5,0	±6,0	±15,0
Digital Resolution (Nm)	0,00025	0,00063	0,00075	0,0019
Stiffness (Nm/rad)	6300	15,000	16,600	39,700
Single-axis Overload (Nm)	14,3	32,8	37,5	86,1
Multi-axis Overload Coefficient, d (Nm)	14,3	32,8	37,5	86,1
M_z				
Standard Measurement Range (Nm)	±2,0	±5,0	±6,0	±15,0
Digital Resolution (Nm)	0,00025	0,0063	0,00075	0,0019
Stiffness (Nm/rad)	1170	3700	3070	9700
Single-axis Overload (Nm)	8,7	26,4	22,8	69,4
Multi-axis Overload Coefficient, e (Nm)	8,7	26,4	22,8	69,4

Figure 11
JR3 Multi-Axis Force Torque Sensor System.

The matrix six by six, of the forces and moments, is multiplied by the column vector shown in the **figure 12**; the result is a calibrated force. It is recommended to have the matrices multiplied by a computer, although manual calculation is possible (**Figure 12**).

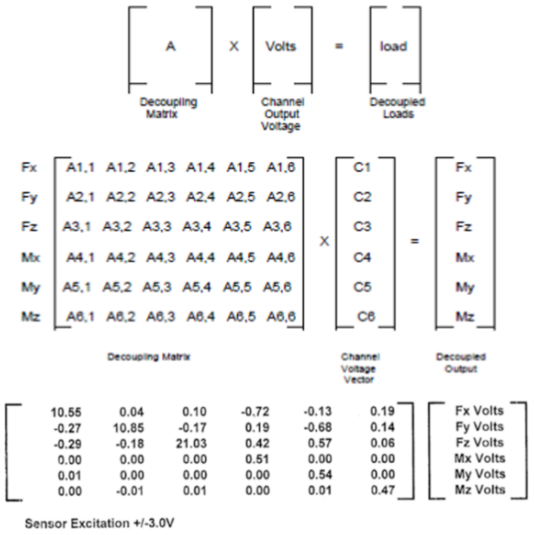

Figure 12
Schematic example of a 6x6 matrix.

Thus, at the output of the sensor, six voltage values are measured, these are multiplied by the calibration matrix in order to obtain forces measured in Newton. The sensor has eight channels, of which the zero channel gives constant values while the channels one to seven return the information object of the study.

The sensor outputs are already converted from analogue to digital and amplified and combined to provide the representation of force data and torque loads for each axis. A low-pass filter, reduces high frequency noise and prevents aliasing phenomena to the analog-to-digital converter.

Therefore, once the data were acquired, the processing was carried out in the MATLAB environment. The minimum of each vector was calculated, corresponding to the maximum peak of force applied in each single test; taking these values in the form, the mean and the standard deviation were calculated. Thus, the mean of the values represented was defined as the force generally imposed by the operator on the eye during the sampling of the ocular surface. The average peak force is 2.08±0.46N.

2.3 Design of the entire kit of the sampling device

The device has a cylindrical shape, like a pen, and has at its upper end a section with a circular base of 17 mm outer diameter and 14,4 mm inner diameter (**Figure 13AB**). This has been designed to position a nitrocellulose membrane with its support, already present in the package itself. Its overall length is approximately 87 mm, allowing a perfect grip in the operator's hand (**Figure 13C**). The weight is about 12 grams. Mounting geometry has been designed to be easily handy for the user and properly sample the ocular surface. The device is disposable. The purpose of this pick-up device is to allow the nitrocellulose membrane, positioned in the upper section of the stick, to take an imprint of the ocular surface, taking from 2 to 4 layers of epithelial cells, both from conjunctiva and/or cornea.

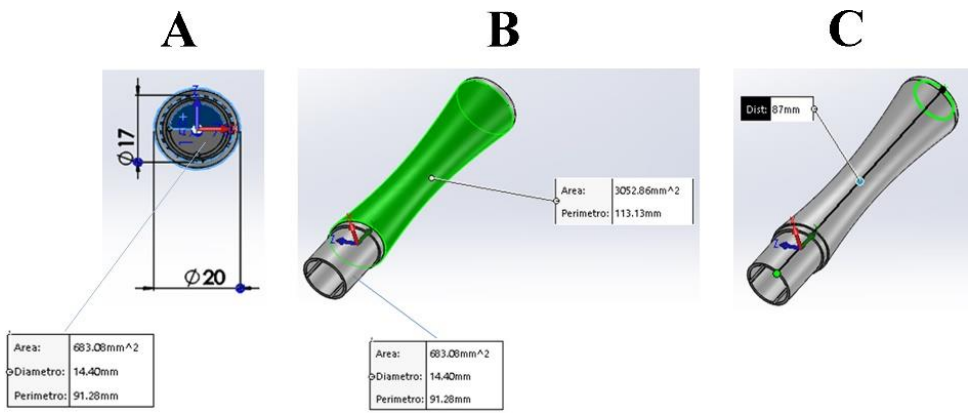

Figure 13
A new and simple ocular surface sampling device.

2.4 Designing the periocular Device B

Periocular Device B acts as a support for the pick-up stick sampling device. It is a periocular system that allows a targeted and reproducible sampling; it can filter tremors or inexperienced movements by the operator. A circular ring-shaped base has been created with an outer diameter of about 49mm and an internal diameter of 44mm to obtain a complete winding of the orbit and not obscure the patient's view.

The external diameter has been designed slightly larger than the orbit in such a way as to firmly rest on the face, partially block the movement of the eyelids and not create a sense of discomfort or constriction in the patient as shown in **Figure 14A**.

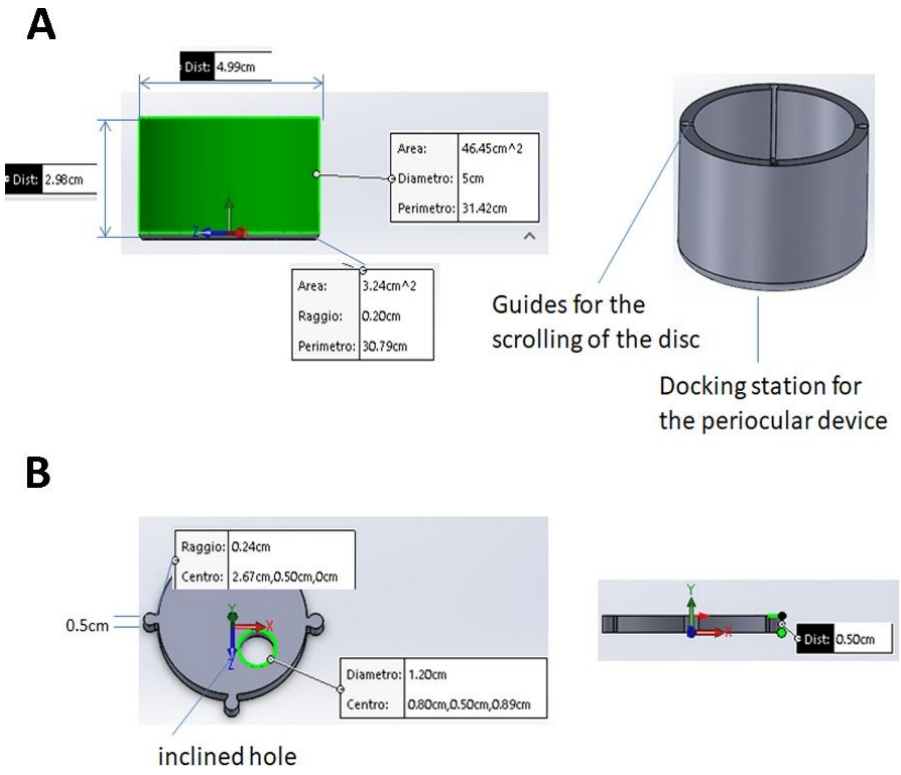

Figure 14
Periocular device B. This device acts as a support and allows a targeted and reproducible sampling.

The height of the device B is approximately 29mm. The weight of the device is about 50 grams apart from the internal springs.

The base of the device B, is arranged for housing a movable disk, which slides inside on four linear guides. The mobile disc has one hole for the insertion of the sampling device, allowing sampling at different points of the ocular surface. The block of the mobile disk of the device B is guaranteed by the presence, at the upper end of the periocular support, of a ring. This has the dimensions of 5 mm of thickness, 49 mm of external diameter and 44 mm of internal diameter (**Figure 14B**).

The presence of the mobile disc on linear guides allows guiding the operator in performing the cytological pickup, by compensating possible tremor or involuntary motions. The use of the properly sized springs guarantees the control of the maximum forces applicable by the operator's hand during imprinting, thus

increasing safety in the interaction with the ocular surface and avoiding tears of tissues.

The hole, present on the mobile disc, is suitable for inserting the pick-up stick element and allowing the sampling in different points of the ocular surface by simply rotating the second additional device as shown in **Figure 14B**. The discharge of the mobile disc from the second element will be favorably avoided by the presence of a circular element fastened to the upper end of the periocular support. According to an embodiment the complete device could have a weight not exceeding 250 grams excluding the springs. The used material, excluding the springs, for creating the device could be for example ABS material, that guarantees the possibility of sterilizing in autoclave (as Tg=150°C), or by means of gamma rays.

This periocular device B has four linear guides arranged at 90° each other for housing a mobile disc sliding along the hollow cylinder of the main body of the element. Four compression springs, positioned in the linear guides, have the following features: inner diameter equal to 2.55 mm, outer diameter equal to 3.05 mm, free length (if not subjected to load) equal to 20.57 mm, length at compaction equal to 7.75mm. The four springs have a stiffness, K, equal to 0.16 N/mm and they result to resist to a maximum force equal to 2.14 N, measured experimentally during imprinting procedures performed in laboratory.

Compression helix springs have been chosen because they are used to withstand direct stresses according to the axis of the cylinder on which the helix is wound; under the action of such forces, the principal stress to which the thread is subjected is torsion.

The relationship between applied force and inflection of the spring is of the type:

$$F=F(\delta,E,I\text{-}n\text{-}L) \qquad T=T(\beta,G,I\text{-}n\text{-}L)$$

where

F - T: correspond to external force - external torque

δ - β: correspond to the movement - rotation

E - G: correspond to the normal-tangential elastic module

I-n-L: correspond to the geometric parameters

The spring stiffness is generally expressed as:

$$K=\partial F/\partial \delta$$

and depends on the elastic module of the material and the geometry of the spring. This was considered constant; the spring therefore results in a linear force-displacement relationship.

Therefore, the stiffness will be calculated as:

$$K=G\frac{d^4}{8nD^3}$$

D: indicates the average diameter of the loop, defined as the mean value between external and internal diameter

d: indicates the diameter of the wire

n: represents the number of active turns, therefore not considering the terminal turns that do not intervene in the deformation because in contact with the end plates

G: module of tangential elasticity for steel, equal to 78400 MPa

The calculation of the elastic constant was made considering:

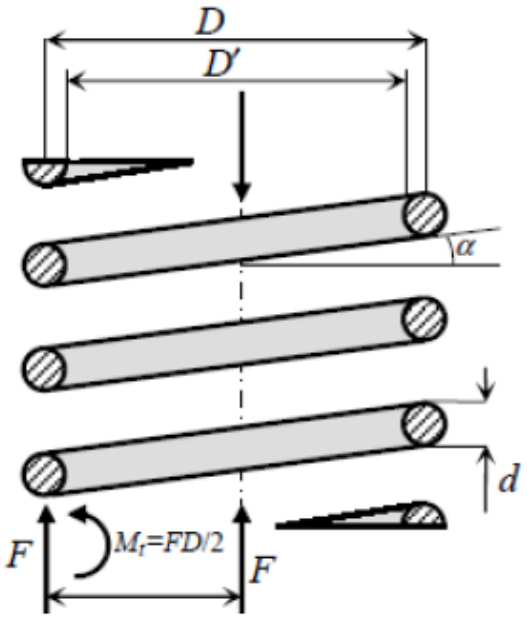

d: 0.3mm

n: 10

D: 2,9mm

K = 78400 $\frac{0.3^4}{8*10*2.9^3}$ = 0.32$\frac{N}{mm}$

Hence, we need springs with constant elastic K which does not exceed this value. The four springs are arranged in parallel and we assume they are subjected to the same strength for simplicity of calculation.

Under the action of the force F acting along the axis of the cylinder all the sections of the spring, equally oriented with respect to F and equidistant from its line of action, are stressed in the same way that the cylindrical propeller spring with constant pitch is a uniform solid with respect to the load F. The generic section is stressed from the normal and tangential components of force F and bending components e twisting of the moment F=$\frac{FD}{2}$ of the same force.

You get:

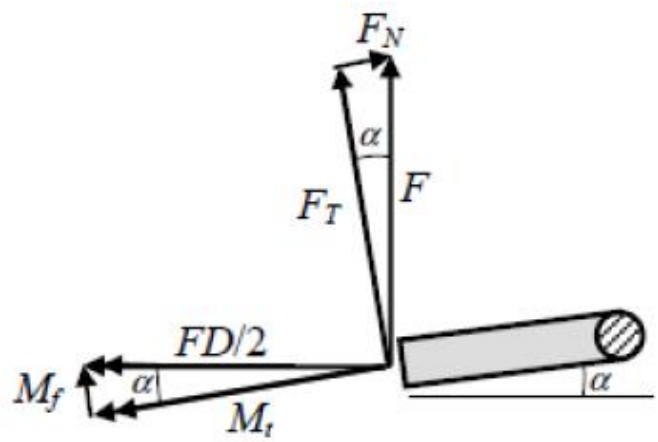

$F_N \approx 0$ e $F_T \approx F$

$M_f \approx 0$ e $M_T \approx \frac{FD}{2}$

Considering α sufficiently small.

The maximum tangential tension in the wire due to the torque and the cut can be calculated according to the equation.

$$\tau = 8\frac{FDd}{\pi d^3} + \frac{4F}{\pi d^2}$$

$$\tau = 8\frac{2.08*2.9*0.3}{\pi*0.3^3} + \frac{4*2.08}{\pi*0.3^2} = 200.25\text{MPa}$$

Being the wire with a circular section of diameter d; τ therefore represents the cutting tension in the internal fiber of each spring.

The material of the springs is stainless steel, DIN 17224 AISI 302 Werkstoff NO. 1.4310; the working temperature is between -200 ° C and +280 ° C, DIN 17224 AISI 302 WERKSTOFF NO. 1.4310. These were ordered from Sodemann Industridjedre A / S, Industrivej 21, 8260 Viby J. Denmark.

2.5 Closing Element of the pick-up Device

The pick-up stick has a closing element, that has different functions. The main function is capping the stick and protecting the membrane from any contact with the outside that is not the ocular surface. The second function is to contain a specific solution for biochemical analysis that will be carried out later. This solution can be for proteins or nucleic acids extraction, or a fixative for the membrane, so as not to allow the degeneration of the epithelium withdrawn and therefore unusable for any eventually microscopic analysis. This is completely adapted to the form of the stick. The shape of this container has been designed like the cap

of a pen, in fact it allows the complete closing of the final part of the pick-up stick, to which the membrane with its support is attached. Therefore, once the sampling device, after the ocular impression, has been inserted, the membrane will be completely immersed in the solution even if the whole assembly is turned upside down. The distance from end to end of the closing element from the central part is of 40.15mm as shown in **Figure 15A**. To permit the stand-alone upside down of the sampling stick, the closing element is composed of two portions, the upper portion that contains the liquid extraction solutions or fixative solution, while the lower portion has a slightly flared base to allow the device to stand up on its own. The upper portion has a perimeter of 121.26mm and an internal area of 1165.78mm^2 in order to allow to contain about 300µL of solution, while the lower part of the support has a perimeter of 127.55mm. **Figure 15B** shows the whole kit assembled.

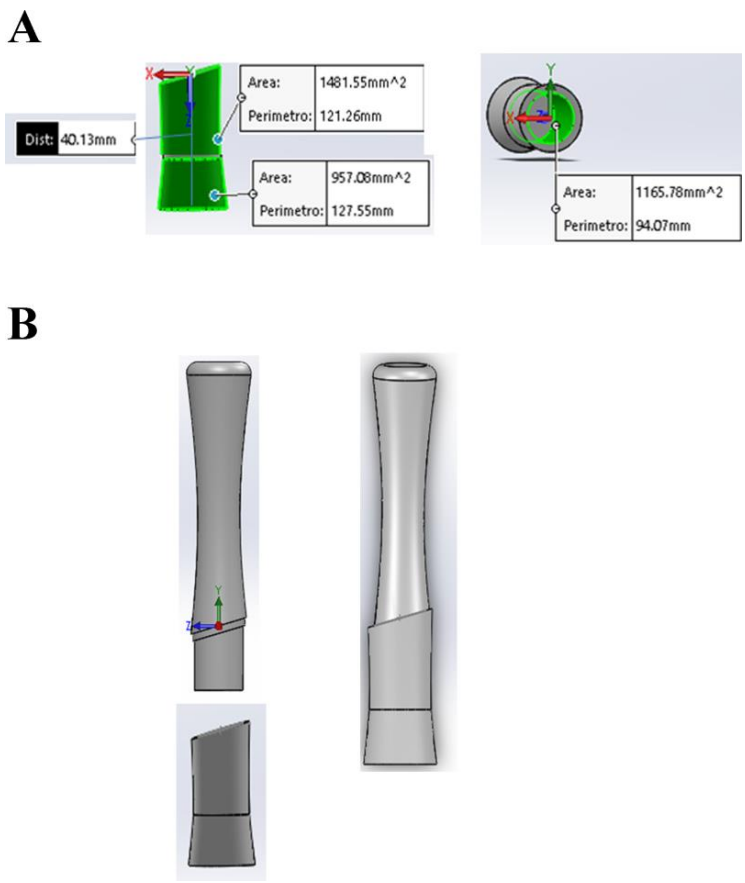

Figure 15
New sampling device kit assembled.

2.6 Prototype Fabrication

The device was produced with rapid prototyping methods with Polijet technology. The Stratasys 3D CONNEX 350 printer was used. This printer uses a photo-polymer jet, layering resins with layers of 16µ and 30µ. This printer provides a print precision of 0.1 to 0.3 mm.

The prototype was fabricated in "ABS Digital-30 micron slicing material" (**Table 1**). The device is disposable. The next steps will be Biocompatibility tests, conducted in compliance with the principles of Good Laboratory Practices (GLP) and / or with reference to ISO / IEC 17025.

Properties	ASTM	Metric	
breaking load	D-638-03	MPa	51
Elasticity	D-638-04	MPa	2192
Elongation	D-638-05	%	18
flexural strength	D-790-03	MPa	80
flexion form	D-790-04	MPa	2286
Resistence	D-256-06	J/m	24
Shore proof	Scale D	Scale D	83
Rockwell proof	Scale M	Scale M	81
heat distortion at 0.45 Mpa	D-648-06	°C	47
heat distortion at 1.82 MPa	D-648-07	°C	43
Tg	DMA,E^	°C	63
ashes contents	USP 28	%	0.005
water absorption	D-570-98 24hr	%	1

Table 1
ABS Digital 30 material characteristics.

2.7 Validation

Conjunctival imprinting, therefore, allows to obtain well-preserved, non-contaminated samples, which can then be evaluated according to different parameters: cellularity, nucleotide-cytoplasmic ratio, presence of cellular categories (Inflammatory and mutagenic cells) and pathogens (bacteria, viruses, mycoses). Impression cytology also provides information on the relationship between the various epithelial elements and allows to highlight alterations

including intra-cytoplasmic (characteristic of chlamydia), loss of intracellular adhesions and nuclear lesions (typical of viral infections), while maintaining unaltered Cell-cell bonds. On the Millipore filters, it is also possible to perform immunofluorescence or immunoperoxidase techniques.
Validation of the device was carried out by a questionnaire and a prototype evaluation on a sample of nine physicians and three biologists after explaining how it works and how it is used; simulating the impression cytology procedure on a dummy test; then it was passed to experimental validation on three volunteer subjects and on 10 sclero-corneal rings obtained from donors. The impression cytology procedure was performed by a specialized medical doctor.

The use of a standardized method greatly contributes to reduce the possibility of error by the operator and enables simple, correct sampling and sufficient cell population, even for those who are less experienced or who can interfere with particularly anxious patients.
After providing a brief description of the device and its use and taking a direct view of the prototype, it was required to fill out the questionnaire by assigning a score from 1 to 5 for each question, where 1 is inadequate and 5 is good. The evaluation questionnaire was organized by dividing the 12 questions between the sampling device A, the subsystem B (Periocular device B) and both paired.

The questions asked were:

- How much is necessary a cytological sampling during an outpatient visit?
- is Device A handy?
- is Device A light?
- is Device A ergonomic?
- is the periocular device B easy to handle?
- is the periocular device B light?
- is the periocular device B ergonomic?
- is the use of device A simpler than the one currently used?
- is the use of the device A + periocular device B simpler than the one currently used?

- is it easy to understand the shape of the instrument and its use with the explanations above?
- does the proposed method more effective than the current one?
- does the proposed method reduce the possibility of error?
- Any comments.

2.7.1 Wet Lab procedures

For *ex-vivo* experiments, sclero-corneal ring not suitable for corneal transplantations were obtained from the Eye Bank of the Hospital of San Giovanni, Rome, Italy and used to obtain initial samples of the human donor ocular surface. The median age, of the patient that have donate their eyes for transplantation, was 70.25 (range, 65–75 years); patients included 5 females and 5 males.
Sclero-corneal rings, from healthy donors, have been used to validate the sampling device, performing more impression cytology's of the corneal and conjunctival area. Briefly, sclero-corneal rings were fixed on a support of a contact lens thus blocking all possible movements of the tissue. Subsequently, 5 samples were taken per zone of the entire sclero-corneal ring (4 conjunctival and 1 corneal) with the sampling device A and the combination of device A plus the periocular device B as shown in **Figure 16**. Immediately after each impression cytology, the membrane was fixed with a specific fixative (Cytofix, Bio-Optica) and placed to dry. This procedure is carried out after each withdrawal. As soon as the membranes are dry, different analysis can be performed based on the biomarker of our interest. The membranes can be treated for histology, PAS staining - optical microscopy, or even for immunofluorescence - confocal microscopy. The procedures used for the different staining's of the membranes will be briefly described below.

Figure 16
Wet Lab sampling

2.7.2 Healthy Subjects

Currently the device has not yet been certified, moreover, an ethics committee is being prepared at the Campus Biomedico of Rome, in order to use the device in the clinic. For this reason, only three samples were taken from three volunteers who are part of the patent in order to have some preliminary tests. The median age was 30.5 (range, 27–37 years); patients included 2 females and 1 male. Staining of the Samplings obtained are described in the result section.
An impression cytology was taken from the left eye and one from the right eye with the different methods.

The first method consists in applying the Millipore membrane without the aid of any support. This method has been difficult for the operator since the support of the Millipore membrane, is very smooth and small, and the physician, by gripping it, obscures the eye of the subject with his right hand, while the other hand should keep the eyelids open (**Figure 17A**).

The second method consists in applying the new sampling device. Thus, the physician has been able to perform a more targeted sampling, keeping away from

the eye and having only two fingers to hold the device without difficulty (**Figure 17B**).

The volunteer does not accuse any annoyance from the approaching device and feels only a slight pressure. The proposed method is completely painless.

The third method consisted in applying the new sampling device accommodated in the periocular device B. The physician performed a good sampling, blocking the eyelid with the device and holding the sampling pick-up stick without difficulty (**Figure 17C**).

The volunteer exposed a slight discomfort with respect to the periocular device B, being directly in contact with the ocular orbit and considerably reducing the 360° vision. The proposed method is painless like the pick-up stick.

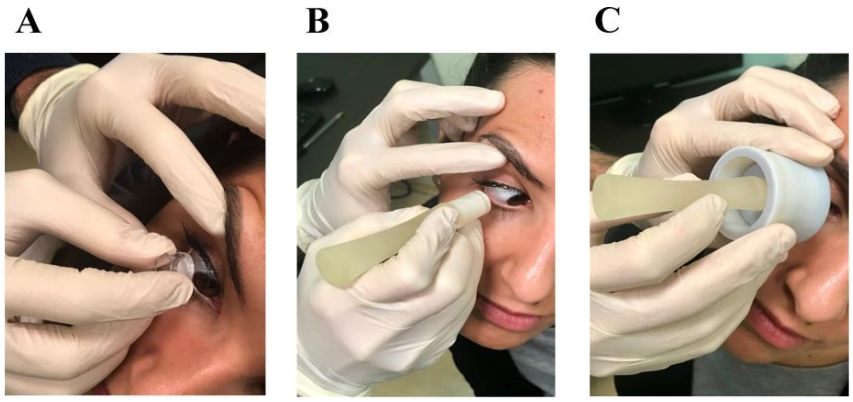

Figure 17
Ocular surface sampling.

The samples were taken directly to the IRCCS Ophthalmology Laboratory G.B. Bietti Foundation for staining techniques.

2.7.3 PAS staining

The cytological sample analysis is the PAS (Schiff periodic acid - reactive acid) staining, a chemical reaction that highlights, in magenta red, tissue components marked by adjacent glycolic or amino-hydroxyl groups. The most highlighted components of this technique are glucidic glycogen, basal membrane, mucin and heparin.

The PAS staining (Periodic Acid Schiff Hotchkiss - McManus # 04-130802, Bio-Optica) steps are directly made on the attached membrane anchored to the plastic support. The impression cytology's are first moistened in distilled water for 3 minutes, first we add 3 drops of the Periodic Acid reagent to 1% for 5 minutes, an oxidative acid that oxidizes aldehyde groups, after a brief wash in distilled water for 1 minute, other 3 drops of the Schiff base reagent are added for 2 minutes, a basic sulfuric agent, that reacts with two closely contiguous aldehyde groups forming the one that is a Schiff leukobase. Membranes are again washed in distilled water for 3 minutes and nuclei are counterstained with 3 drops of Hematoxylin reagent for 2 minutes, a substance having an empirical formula $C_{16}H_{14}O_6$ which is extracted from the Haematoxylum campechianum plant and colors the nuclei blue-purple, to differentiate and brighten up the membranes are washed in source water for 5 minutes then balanced in phosphate buffer. After the PAS staining, membranes are removed from the plastic support using a lancet and placed on a slide and closed with the use of glycerol / gelatin dissolved in buffer phosphate.

The results obtained by PAS staining for Goblet cells visualization are shown in **Figure 18**.

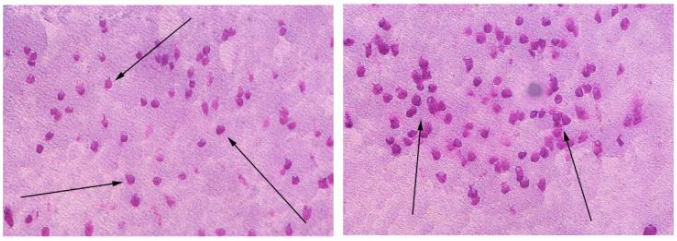

Figure 18
PAS staining of an impression cytology. Goblets cells are visible in magenta. The number of mucin secreting cells are index of healthiness of the ocular surface.

Membrane observation was performed using a Direct Light microscope that transmits directly to a computerized camera and images are analyzed by an Imaging Software NIS-Elements program (Nikon, Tokyo, Japan).

2.7.4 Confocal Microscopy

For immunofluorescence, sclero-corneal rings of eye globes from donors were fixed by Cytofix. Membranes were first treated with 0.05% Triton x100 (Tx100) in PBS and after 2-times wash (5 minutes each) incubated overnight at 4°C with the following antibodies: monoclonal mouse anti-Muc5AC (1:100; Santa Cruz), polyclonal goat anti-CK19 (1:100; Santa Cruz), polyclonal rabbit anti-CK3 (1:100; Santa Cruz) and monoclonal mouse anti-CK12 (1:100; Santa Cruz). After washing with TW-PBS, the sections were incubated for 1 hour at room temperature with Alexa Fluor 488 donkey anti-rabbit IgG (1:200), Alexa Fluor 638 donkey anti-goat IgG (1:200) and Alexa Fluor 555 donkey anti-mouse IgG (1:200), all purchased by Thermo Fisher, (Massachusetts, USA). After 2-rinses in TW-PBS and 10 minutes incubation with the TOTO3-Iodide for nuclei visualization (0.1 mM TOTO3; Molecular Probes, Invitrogen, Italy) or Iodium Propide, the sections were examined under a confocal laser scanning microscope (Nikon C1, japan) under sequential mode to avoid crosstalk between channels as shown in **Figure 19**. The confocal image acquisition was conducted so that all samples were imaged using consistent settings for laser power and detector gain. No intensity-image adjustment was carried out and the panel assembling was performed using the software "Adobe Photoshop".

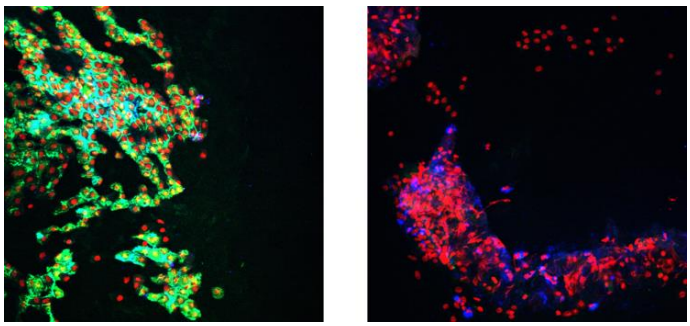

Figure 19
Example of fluorescent staining of an impression cytology. Different staining of cytokeratin's present on the ocular surface.

2.7.5 Statistical analysis

All experiments were performed in triplicate and data were provided as mean±SEM in the graphics. Unpaired Student t test analysis was performed using GraphPad Prism package for Windows depending on the data population to compare the different sampling techniques and evaluate the number and the mean average of cells sampled. A p-value ≤ 0.05 was considered significant. The REST/ANOVA-coupled analysis was carried out for molecular comparisons.

2.8 Results

2.8.1 Questionnaire results

The respondents are happy to accept and are very interested in using the device as exposed in **Table 2**.

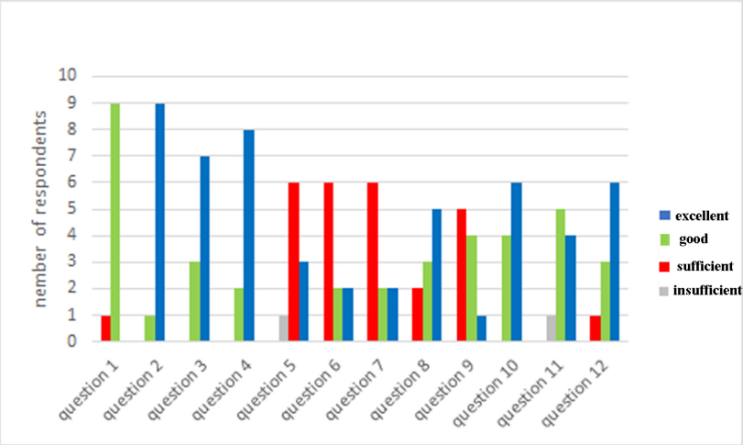

Table 2
Prototype evaluation questionnaires.

85% of the surveyed operators recognize the device as lightweight, ergonomic and manageable, are interested in its possible use and have nothing to criticize on its shape and features.

60% of the consulted operators, on the other hand, show little interest in subsystem B, or periocular device B, as it is bulky and geometrically not ideal to use; though they recognize a potential improvement in efficiency and simplicity of the sampling procedure.

Overall, approximately 70% of the operators surveyed are satisfied with the proposed device and evaluate its use, giving a good overall judgment.

2.8.2 Analysis and Validation of the Results

The experimental validation of the devices was evaluated by a team of 3 biologists and a physician experienced in processing pre-analytical and analytical impression cytology, analyzing images resulting from the PAS staining of the membranes obtained in wet-lab on sclero-corneal rings, from donors, or from membranes obtained from the three volunteers.

- First method: Millipore membrane

As already shown by previous studies on the Millipore membrane, the epithelial cells population (blue/violet) and Muciparous cells (fuchsia) are sufficient and the analysis is valid (**Figure 20A**).

- Second method: new sampling device

Epithelial cell population is more abundant, well-distributed, and cells are more distinguishable (**Figure 20B**).

- Third method: pick-up stick combined with the periocular device B (A+B).

From the membranes obtained using the two combined systems, the cellular population is less well-distributed, as compared to the single Millicell or SurfAL membranes (**Figure 20C**).

Consistent with the results obtained in immunohistochemistry, the results attained in immunofluorescence show the presence of the Muc5AC, in green in the lower squares in **Figure 20**, expressed by the goblet cells of the conjunctiva. As noticeable, from the different images gained from the three different sampling methods, the impression cytology's obtained with the new sampling device, the Muciparous cells are more abundant and visible than those obtained with the

simple Millicell membrane or in combination with the periocular device B (**Figure 20**).

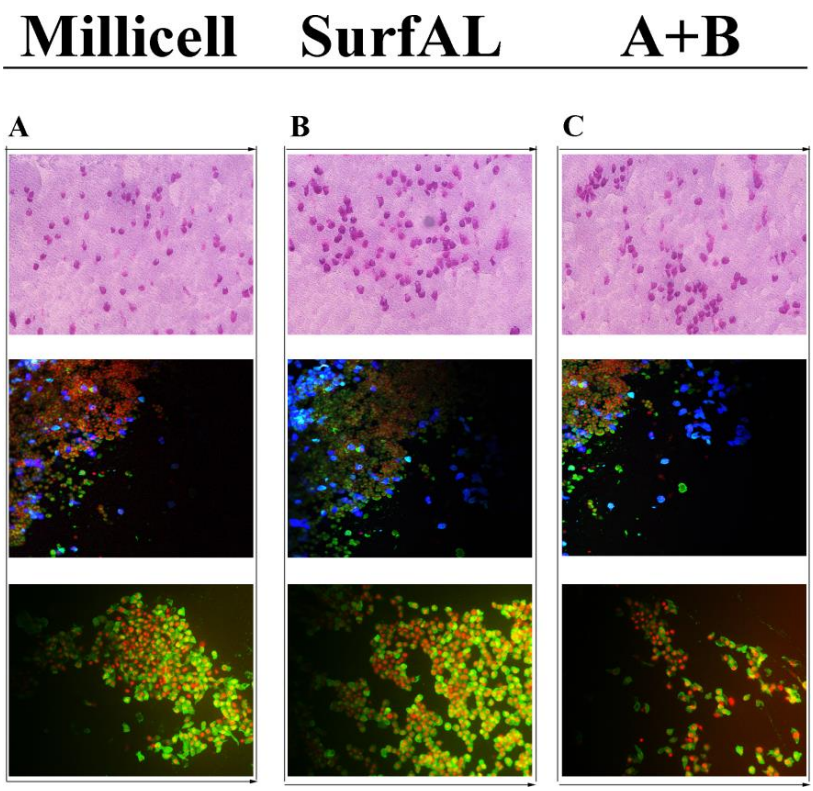

Figure 20
Impression cytology obtained from three different methods and stained for PAS (upper panels), CKs (middle panels) and Muc5AC (lower panels).

Mean differences of Goblet cells were normally distributed (n=16 Millicell= 26.89±6.04; n=32 sampling device= 36.82±8.12; n=16 periocular Device B= 28.32±7.39). The analysis by group showed a significant difference ($p < 0.001$) on the reported means of the sampling device with respect to the Millicell sampling. No significant differences were seen between the Device B and the Millicell ($p > 0.05$) and a slight significance between the groups sampling device and periocular Device B ($p < 0.05$) as shown in the graph **Figure 21**. The sampling device was the only group to have a 95% confidence interval above zero 13.15%.

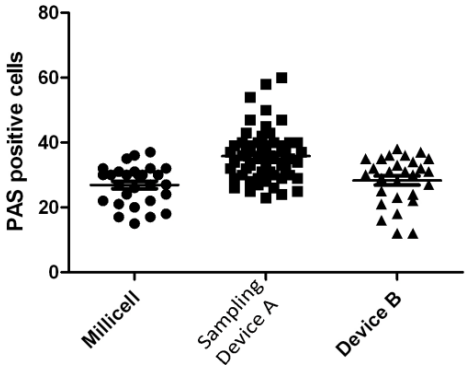

Figure 21
plot graph representing the positive goblet cells obtained with the three different sampling methods.

About the impression cytology's carried out on the volunteers a comparison was carried out between, the Millicell membranes, the new sampling device, the pick-up stick combined with the periocular device B and finally the EyePrim as shown in **Figure 22**.

Getting results very similar to those obtained in wet Lab, and certainly better than the colored membranes of EyePrim. In the case of the EyePrim™ the sampling is partial and does not seem easy to realize because the device is not "ergonomic" and therefore does not completely replace the classic method with Millicell support (Millipore membrane). The reluctance would lie in the fact that the syringe device is not manageable at the time of ocular sampling. In this regard, the new sampling device provides an improvement both in the classic outpatient sampling (Millicell) and in comparison, with the EyePrim™ method.

The colors were made in parallel in order to minimize the "variability" component operator/reagents ".

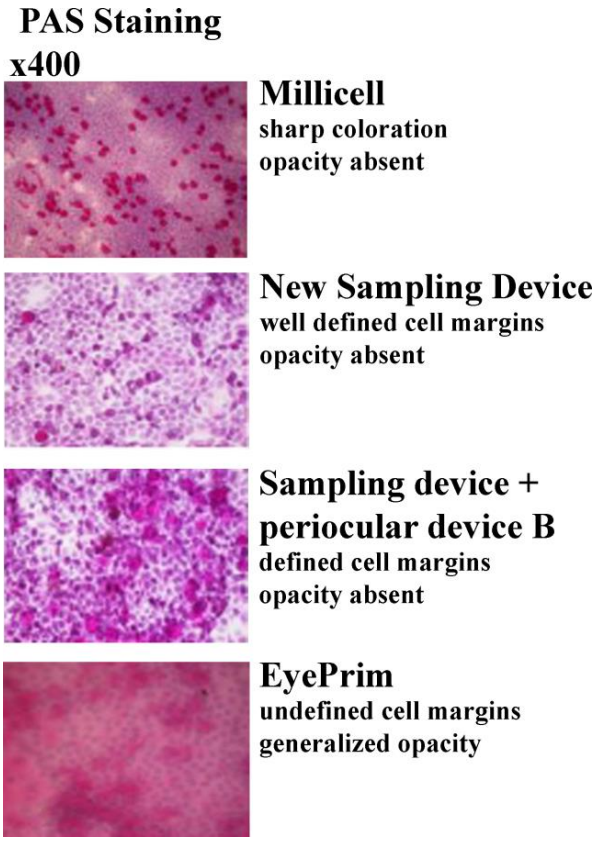

Figure 22
PAS staining comparison between different sampling methods.

2.9 Conclusions

Finally, the development of new sampling devices could reduce the gap with the concept of personalized medicine. These new devices would reduce the response time, hence the diagnosis of the doctor. So, for this reason my thesis, which aims at the discovery of specific biomarkers for different ocular diseases, proposes the development of a new sampling device of the ocular surface, capable of withdrawing 3-4 analyzable layers of cellular epithelium. The advantage of this research thesis was to ensure rapid diagnosis, a condition of extreme utility especially in the field of ophthalmology, especially if applied to retinal disorders, where a slight damage may, if not timely and accurately treated, bring to blindness. Therefore, qualitative and quantitative analysis in the outpatient clinic is extremely useful. The development of this new sampling device, would therefore, provide support for the ophthalmic investigation, especially in the case

of a controversial diagnostic doubt or framework, and would allow monitoring the course of a pathology and/or therapeutic treatment.

Next step will be to find positive feedback when proposing the device to the doctors concerned, regarding its flexibility in outpatient care and not only. As well as suggesting the device to healthcare providers such as ASL (Azienda Sanitaria Locale), present in the territory, which boast many users, use it and later create a national database where you can keep anonymously all the data provided by it. These could therefore be used in research laboratories to monitor the progress of pathologies and develop appropriate care in the future.

The results obtained in wet-lab and then on the three volunteers confirm our hypotheses on the validity of this sampling device about the final evaluation of the sample. There is a sufficient cell population with well-defined cellular margins, we got an appropriate staining, thanks to a clear membrane that doesn't present opacity and therefore there is a concrete reproducibility. While for the periocular device B, the results are very similar to those obtained with the sampling device, but it influences, according to the respective physicians who carried out the sampling, that the device is slightly bulky for the patient and makes the sampling of the ocular surface a little more difficult. But at the same time, it reduces the possible tremors of the operator's hand, and therefore the possibility of obtaining unverifiable samples and thus also inflicting the final diagnosis.

In conclusion, the device, which is the subject of this study, brings an improvement to the technique based on a simple support of the material already tested and validated by different laboratories and research centers, PAS positive cells are more reliable, and thus the diagnosis of dry eye, for example, may be promptly treated with eye drops. With this device other pathologies of the ocular surface like Acanthamoeba or limbal deficit are diagnosable in office and hence, a minor cost for the ASL is predictable.

CHAPTER 3

A new constitutive element of the ACkit

Abstract

Corroborating data suggest the significance of the study of biological fluids for the research of biomarkers specific for a pathological state. Body fluids are highly complex mixtures containing a variable concentration of cells, proteins, macromolecules, metabolites and small molecules. Analysis of body fluids has become one of the most promising approaches to the discovery of biomarkers for human diseases. Hence, my goal was to develop a new element that would progress an already existing patented device, by permitting the solubilization of proteins/nucleic acids in body fluids, or solubilize the cells present on the nitrocellulose membrane of the sampling device described in the previous chapter, for the research of these disease markers. 30 rats and 30 mice were used to analyze and investigate the entire eye and its tissues (cornea, humor fluids or retina). Tissues were homogenized and solubilized in this new element previous to analysis with the current laboratory techniques. Different markers have been found to correlate with some specific eye disorder. In conclusion this new progress element would improve the analysis and therefore the research of new biomarkers in not only biofluids, but also from impression cytology, permitting the researcher to use more different techniques for the same intention.

3.1 Introduction

Tacking advantage of a physiological fluid for non-invasive investigation, one of the main difficulties is to understand and ensure that the analyte concentration in the sample correlates with the known disease biomarker (**Choy CK 2003**). However, by now biomarkers are still not yet considered, due to their not clinical validation. This is justified in part to the lack of methods for validation, verification,

research assay optimization and commercialization. To understand the biological and clinical relevance of biomarkers, an effort should be made in the development of "omics" approaches applied to proteins. In this thesis I will provide a new element that will progress an already existing patented device, which can be identified as new concept of analyzing or testing devices. Once this element concept has been created, an engineering design and development optimization was performed, and at the end a production of a prototype carried out. This new element is very simple, it has been designed in the form of a cap with an upper hollow part to contain an extraction solution, and a lower portion with a spout to allow the flow of the proteins extracted, through a special channel on the membrane of the analysis device. The main function of this element, thus, is the solubilization of the proteins that will be analyzed with the patented device or with the currently in use laboratory techniques.

3.2 Designing the new element

The new element or CAP (**Figure 23A**), will be a component of a patented kit (ACkit), which is made up of a unit composed of a base with a micro vessel from which the biological fluid flows and deposits on a membrane spotted with different targets, on which to analyze any biomarkers present in a fluid sample (**Figure 23B**). Specifically, the new element or cap designed in Solidworks, has a hollow cylindrical shape, with an upper opening for sample insertion and a lower opening for the flow of the extract on an analysis membrane.

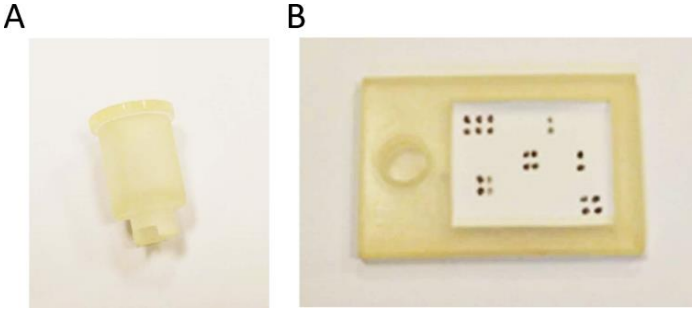

Figure 23
A Prototype of the CAP and **B** the patented device ACkit

The cylindric shape is closed by a plug. The height of the whole element is 20mm and the cavity of the cylinder has a capacity of 300-400µl of extraction solution. The cap has a diameter of 13mm and allows a hermetic seal of the cylinder, so as not to permit the liquid contained in it to fall out as shown in **Figure 24**. The lower opening is sealed by a membrane that brakes in contact with the patented device when inserted in the accommodation space, after the protein/nucleic acids are extracted from the sample and before they drain on the analysis membrane. Therefore, upon extraction, by simple pressure, proteins will be injected onto the membrane spotted with different biomarkers. Hence, this extraction cap, permits the researcher to eliminate some laboratory steps necessary to obtain suitable sample analyzable with the analysis device. As shown in **Figure 24**, with this new element it is possible to extract proteins/nucleic acids from different samples, such as tears obtained with micropipettes, from membranes (Schirmer strips) used to evaluate the amount of tear present in the lacrimal sulcus, biopsy, or even by impression cytology's obtained to evaluate the quality of the ocular surface. All these different sampling methods converge in our new element which in turn may contains a specific extraction liquid, composed of modified RIPA buffer (50 mM Tris–HCl, 150 mM NaCl, 1 % Triton X-100, 5 mM EDTA, 100 mM NaF and 1 mM PMSF; pH 7.5) for protein extraction or TRIFAST a phenol and guanidinium thiocyanate in a monophasic solution, for nucleic acid extraction. Consequently, allows the solubilization and after a simple pressure of the cap, in the appropriate housing, the release of these that will flow to a membrane spotted with different biomarkers of the analysis device.

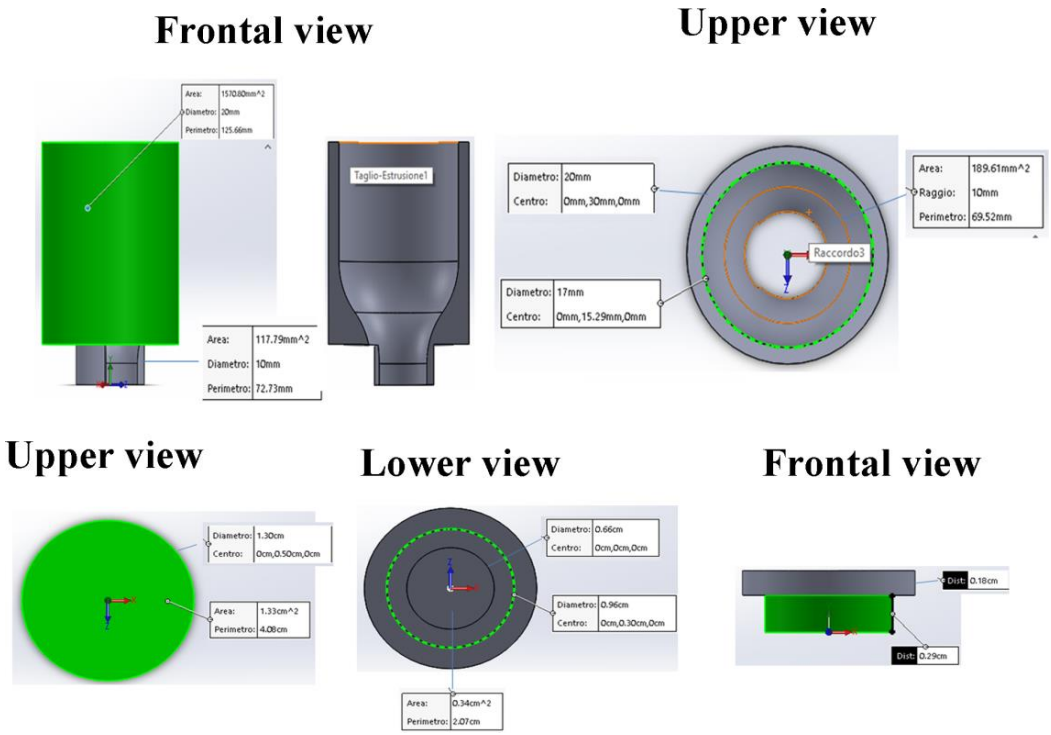

Figure 24
The new element for the patented Analysis Device ACkit.

3.3 Prototype fabrication

For this purpose, prototypes have been printed with a Polijet technology, the Stratasys 3D CONNEX 350 a 3D printer to obtain functional prototypes to test the effectiveness of the CAP in the laboratory and, if necessary, modify the design to make it more reliable. Commercially available material, such as ABS was used to obtain a functional prototype.

3.4 Analytical validation

As reported in literature, there is a need to conceive a less invasive method to self-monitor the state of a disease. Overall, for clinical outcome, it is very important to make available the translation of the advances from benchtop to bedside, with the purpose to give the population a benefit from this investigation, either through new biomarkers discovery for the development of new drugs and through the production of new devices.

As analytical procedures, different laboratory methods have been used to validate the new element. Different animal models were used to asses and validate the project of the solubilizing cap, rats or mice were used to obtain eye samples, for biomarkers quantification and analysis. In particular retinal samples, or vitreous/aqueous humor were analyzed to search and quantify the NGF and its receptors and to verify if the solubilization liquid contained in the cap, extracted in good quantity and quality the proteins. After having collected and solubilized the sample in the cap, the homogenate obtained was tested with techniques such as western blot, ELISA, Flow Cytometry regarding proteins or Realtime PCR as far as nucleic acids are concerned. These techniques, currently used in all research laboratories, allow the analysis of the sample giving a qualitative result, but also in some cases quantitative, of a particular marker. This allows the researcher to determine, starting from a sample, a specific biomarker for a given pathology that is not only ocular, but also referred to other body districts. The ocular samples used for these tests were from animals (rats/mice), or from human donors. Below I will report in detail all the procedures performed on the samples taken and extracted with the cap.

3.4.1 Animal models

All experiments were conducted in accordance with the guidelines for the use of animals stated by the Association for Research in Vision and Ophthalmic Research. 30 Royal College of Surgeon (RCS) rats (at 5 postnatal days), housed at the CNR animal facility and 30 Reeler mice (at 21 postnatal days), housed at animal house facility ("Tor Vergata" University) under standard conditions (12hrs light/dark cycle, temperature 21±1°C and relative humidity 60±10%). Both water and food were freely available (Enriched Standard Diet, Mucedola, Settimo Milanese, Italy). Animals have been used to search different biomarkers for possible diseases afflicting the eye. Eyes taken from these animals, after been subject to anesthesia, were sectioned and used for the extraction of proteins, nucleic acids or ocular surface imprints, and evaluated with the techniques currently in use in the laboratory. All efforts were carried out to limit animal number and discomfort.

Briefly, animals were deeply anaesthetized by intraperitoneal injection of 2 mg/mL ketamine (0.2 mL/10 gr body weight; Ketavet, Gellini Pharmaceutics, Italy) and 0.23 mg/mL medetomidine (0.24 mL/10 gr body weight; Domitor, Orion Corp., Espoo, Finland). Retinas were dissected out from the eyeballs by producing a corneal tissue incision and the removal of the crystalline, according to a previously reported procedure with slight modifications (**Skeie et al. 2011; Balzamino et al., 2015; Figure 25**). The entire surgical procedure was carried out under a dissector microscope (SMZ645; Nikon, Tokyo, Japan) equipped with cold-light optic fibers (PL2000 photonic; Axon, Vienna, Austria).

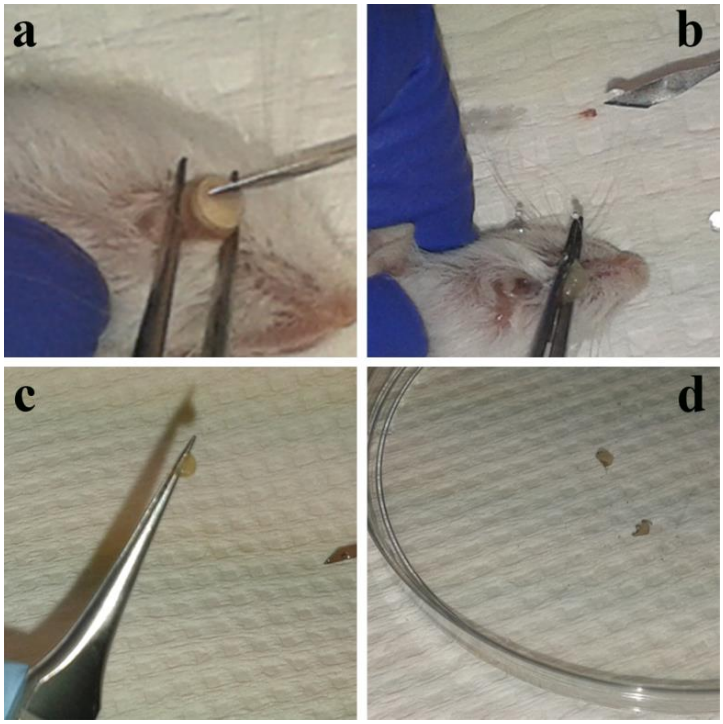

Figure 25
Retina, Vitreous and cornea sampling from mouse eye.

3.4.2 Human subjects

A total of 30 subjects (15M/15F; mean age 57.87±29.14 years old, ranging from 19 to 90 yrs.') were recruited. Inclusion criteria were the presence of co-existing ocular and/or ocular surface diseases, contact lens wearing, systemic diseases (malignancies, dysmetabolism, Psychiatric diseases therapy), pregnancy and/or use of topical as well as systemic medications at the time of examination.

All procedures were performed in accordance with guidelines established by the Association for Research in Vision and Ophthalmology and adherent to the tenets of the declaration of Helsinki concerning human subject contribution. Subjects underwent non-anesthetized tear collection, according to the eye-flush procedure [see **Micera et al., 2016**]. The procedure of sampling comprised the administration of 30µL sterile Balanced Salt Solution (BSS; Alcon Laboratories Inc., Fort Worth, TX) and fast tear collection with a sterile single-wrapped plastic micropipette (PBI Intl., Milan, Italy). Tear samples were quickly preserved by adding a cocktail of protease inhibitors (Pierce Biotechnology, Rockford, IL) and stored at -20°C.

3.4.3 Western Blot

Western blot is used in research to separate and identify proteins. Proteins are separated by molecular weight, and thus by type, through gel electrophoresis. This gel is then transferred to a membrane producing a band for each protein. The membrane afterwards is incubated with specific antibodies for protein of interest. The transfer buffer used is (0,025 M Tris, 0,192 M Glycine, methanol 20% (v/v)). Protein transfer was carried out using a semi-dry blotting apparatus (semi-dry transfer unit, Biorad) set at 45V constant voltages for 1 hour. Once the proteins were completely transferred, the membrane was blocked by incubating at 4°C with a 5% powdered skim milk (w/v) solution in PBS. Next, the primary antibody, diluted in a PBS, was added and the incubation was left for 2-3 hours at 37°C and gently shacked. Before the addition of the secondary antibody, any trace of the primary antibody was removed by washing the membrane 3 times in PBS-Tween 0,05% (v/v) (Tween-20, Sigma-Aldrich) and consecutively 2 times in PBS. The membrane was incubated with the Horseradish peroxidase (HRP)-conjugated secondary antibody at 37°C for 1 hour, and then washed again following the procedure previously described. Finally, the chemiluminescent detection using the enzyme linked chemiluminescence (Femto-ECL) detection reagents (A and B) from Thermo-Fisher was performed. The ECL reagent was incubated on the membrane for 5 minutes leading to catalysis of luminol in alkaline conditions. The luminol in the excited state decays in a chemiluminescent reaction, which was detected by

Chemiluminescence-detector (Kodak) or exposing Kodak films in dark-room. The primary antibodies and the respective dilutions used in this work were: monoclonal mouse anti-TLR2 (1:200; Santa Cruz), polyclonal goat anti-TLR3 (1:100; Santa Cruz), polyclonal rabbit anti-TLR4 (1:100; Santa Cruz), monoclonal mouse anti-TLR7 (1:200; Santa Cruz), polyclonal goat anti-TLR9 (1:100; Santa Cruz). For detection, anti-mouse IgG (DAKO) or anti-rabbit and anti-goat IgG (DAKO) HRP-conjugated secondary antibodies diluted 1:2500 were used (**Figure 26**).

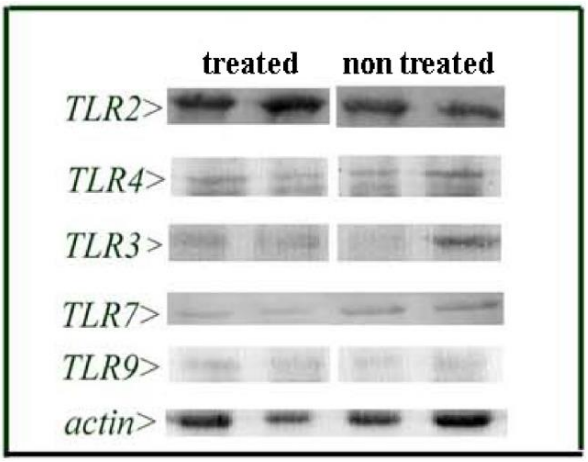

Figure 26
Examples of Western blot analysis of different biomarkers expression in tears samples.

3.4.4 Enzyme-Linked Immunosorbent Assay (ELISA)

Enzyme-Linked Immunosorbent Assay (ELISA) is an antibody application extensively used in many settings, from basic research to diagnostics. This assay is the preferred method to determine the titer of antisera and purified antibodies and can also be successfully employed for the quantitative assessment of an antigen in a sample, often devised in convenient easy to use kit formats. Differently from WB, ELISA allows the detection of proteins in their native folding. Briefly, ELISA Maxisorp plate (NUNC) was coated over-night at 4°C with 100µL with the antibodies desired per well; each sample was repeated at least in triplicate. After blocking with 5% skim milk (w/v) in PBS at 37°C for 2 hours, the plate was washed 3 times in PBS-Tween 0,2% (v/v) and consecutively 2 times in PBS. Next,

the samples, were added and the incubation was carried out for 2 hours at 37°C. The plate was washed again and incubated for one additional hour at 37°C with 100µL of HRP-conjugated-biotinylated secondary antibody, added to each well. After washing thoroughly, colorimetric reaction was developed using 2,2'-azino-bis (3-ethylbenzthiazoline-6 sulphonic acid) substrate (TMB, eBioscience) and read at 450 nm on an automated ELISA reader (Sunrise, Tecan). IL6 ELISA expression is shown in **Figure 27**.

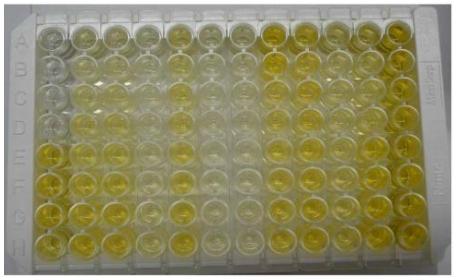

Figure 27
ELISA assay and expression of a biomarker in biological fluids obtained from the CAP.

3.4.5 Flow Cytometry (FCM) Analysis

To release from retinas of rats/mice, a total ''undamaged'' single cell suspension, a Neural Tissue Dissociation solution was used (Miltenyi Biotec; Bergisch-Gladbach, Germany). The cells were collected by centrifugation (3500 rpm/7 min) and equilibrated in cold Hank's balanced salt solution without Ca^{2+}/Mg^{2+} supplemented with EDTA (HBSS; Lonza, Basel, Switzerland). The total cell suspension was quickly post fixed in 0.2 % buffered PFA–HBSS, gentle permeabilized in 0.1 % saponin–HBSS and subjected to specific immunolabeling. Single cells (glial cells, RGCs or RBCs; n=9 eyes/E-Reeler and n=12 eyes/E-control) were equilibrated in HBSS–EDTA supplemented with 0.8 % BSA and probed with the following antibodies: anti-NGF (sc-549, 1 µg/mL), anti-$trkA^{NGFR}$ (sc-118, 2 µg/mL), anti-$p75^{NTR}$ (sc-6188, 2 µg/mL) and anti-Bcl2 (sc-7382, 2 µg/mL), all from Santa Cruz Biotech (Santa Cruz, CA). Labeling was carried out by using the PE-, PerCP- or APC-coupled specie-specific IgG antibodies (1:500-700; raised in donkey; Jackson ImmunoResearch Europe Ltd, Suffolk, UK). Isotype control staining and

single and double fluorescent staining were run in parallel for each set of experiments. Acquisition and analyses were carried out with the MACSQuant Flow cytometer (Miltenyi Biotec). Both linear and logarithmic signals were acquired from 204 cells. Preliminary pilot studies were performed to set up the entire procedure and are shown in **Figure 28**. The acquisition settings were optimized on representative small group of E-Reeler and E-control mice (**Balzamino et al., 2015**).

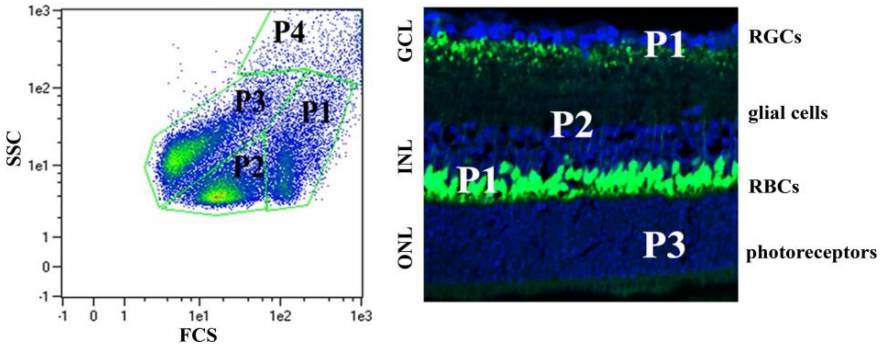

Figure 28
Preliminary data on single cells obtained from retina dissociation. On the right a cytofluorimeter plot displaying single cells based on their size and complexity, on the left an immunofluorescence staining of mouse retinal layers.

3.4.6 Statistical analysis

All experiments were performed in triplicate and data were provided as mean±SEM in the graphics. The two-tailed Student's t-test was used to compare means of two different groups; ANOVA and the Tukey's multiple comparison test were used to study differences of means of multiple samples. A p-value ≤ 0.05 was considered significant. The REST/ANOVA-coupled analysis was carried out for molecular comparisons.

3.4.7 Solubilization and validation of the sample with the CAP

Through the cap, different sampling techniques of the ocular surface can be used as shown in **Figure 29**. From these samplings a single procedure is performed that

leads to the marking of the different biomarkers spotted on the membrane and is visible in **Figure 30**.

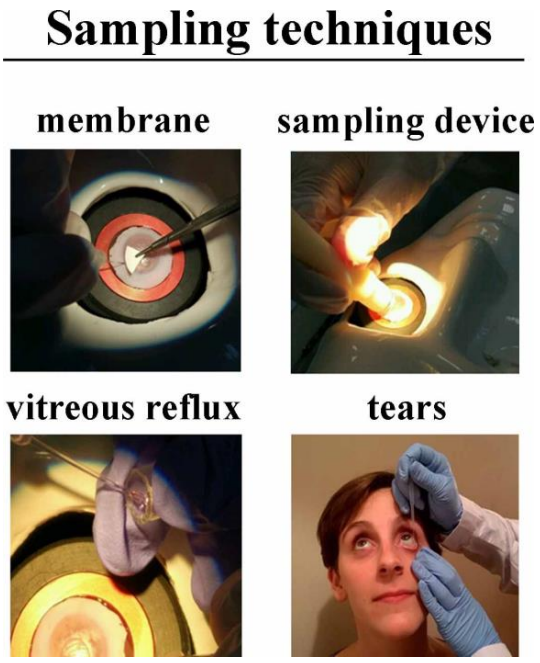

Figure 29
Different sampling techniques may be used to obtain suitable samples for the extraction of proteins with the CAP.

The first step is the solubilization of the proteins, present in the samples, with the extraction solution (0.3 ml final volume) contained in the CAP. Before to drain the sample on the nitrocellulose membrane, a brief blocking process with 5%BSA for 20 minutes of the membrane is performed. The subsequent step is to let flow out from the CAP, the solution containing the proteins on the customized membrane spotted with different biomarkers. The analysis device with the membrane will rest to permit the binding of the proteins to the respective biomarker for at least 30 minutes in an humified chamber for 1 hour. The next step, after three washes in PBS-Tween of the membrane, is followed by an incubation step with Biotin-Conjugated antibodies (1 ml), for 1 hour at 37°C. The last step of the entire procedure is an incubation step with the HRP-conjugated Streptavidin (1 ml/1000-fold dilution), this phase permits the next step, consisting in a chemical reaction with a luminol solution between the Horse Radish Peroxidase (HRP) and the luminol. This permits the visualization of the marked spots on the membrane

thanks to chemiluminescence with a kodak instrument imaging. The acquisition, is a time exposure in a black chamber, the presence of biomarkers, are visible like black spots on the nitrocellulose membrane (**Figure 30 lower panel**). As shown in the figure below, there is an image of a membrane customized for our laboratory, containing several markers of inflammation of interest for eye diseases, growth factors, and other markers that may be of interest in the monitoring of a disease and therefore of help to the doctor in the prescription of specific drugs. The image on the side instead shows an example of a spotted membrane and marked with the technique described above, which displays only the markers present and shows the intensity of expression. This means that a marker of a pathology could be present or not, but also expressed in different quantities, synonymous with gravity or absence of disease, diagnosed primarily by the researcher who transmits the result obtained to the doctor, who in turn will prescribe a medication appropriate for the patient.

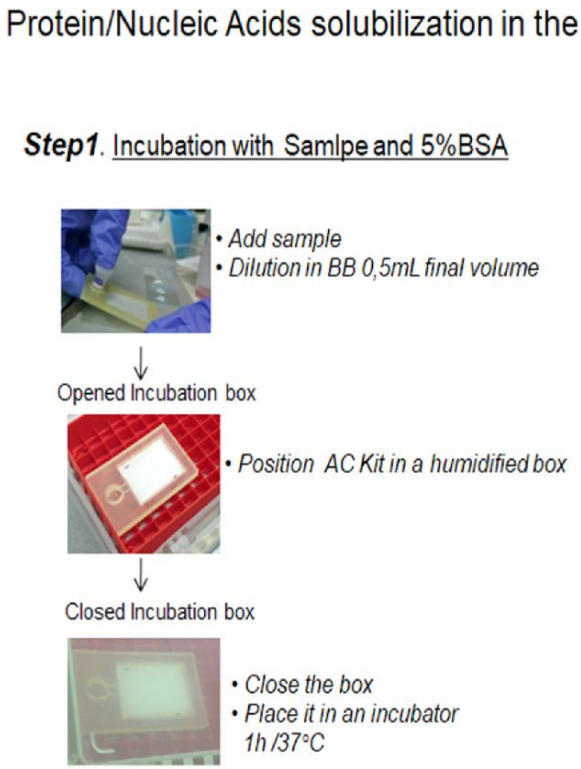

Figure 30

Laboratory procedures, from the protein/nucleic acid extraction to the analysis of the membrane in chemiluminescence and biomarker discovery. Example of a membrane spotted with different biomarkers specific for different eye disorders.

3.5 Results

3.5.1 Preliminary results

Thanks to the use of the CAP, different techniques were undertaken to verify the NGF-trkA^{NGFR}/p75^{NTR} expression in retinas from *E-reeler* mice, a Reelin-deprived model, showing a severe structural and functional changes in the retina. The principal finding of this study is the significant increase of NGF all over the *E-reeler* retina, mainly localized in the layers populated by RBCs (INL) and RGCs (GCL). (**Balzamino et al, 2014,2015; Kim YS et al., 2013**). Moreover, the p75^{NTR}, a pan-neurotrophin receptor, was overexpressed on RGCs of reeler mice as shown in **Figure 31**, while a slight down-regulation of the other NGF receptor trkA^{NGFR} was observed. These findings extend our previous observations on the protective role of topical NGF application on degenerating RGCs and provide both *in vivo* and *in vitro* evidences of a protective NGF role on Reeler mice.

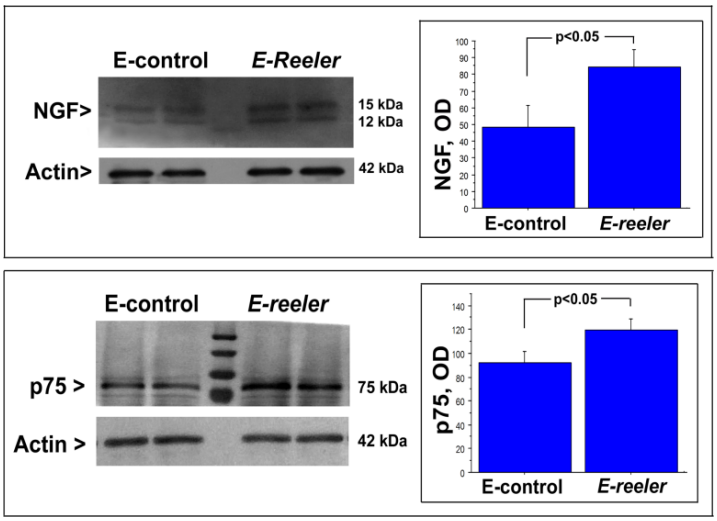

Figure 31
NGF and p75 expression in reeler mouse retina.

A further result obtained using the cap, analysing the solubilized proteins in this new element, with different laboratory techniques, corneas and retinas of RCS rats, an animal model that develops a spontaneously inherited Retinitis Pigmentosa, a photoreceptor retinopathy, have shown similar results to the

mouse reeler. To clarify whether photoreceptors might be a target for NGF, both trkA^{NGFR} and p75^{NTR} expressions were verified *in vitro*. Whole retinas from 10-day old RP rats were digested to release total single cells, as shown in **Figure 32**, high trkA^{NGFR} expressions was observed in isolated photoreceptors stained with Rhodopsin unlike the first animal model, the trkA^{NGFR} receptor increases in photoreceptors (**Rocco and Balzamino, 2015,2017**).

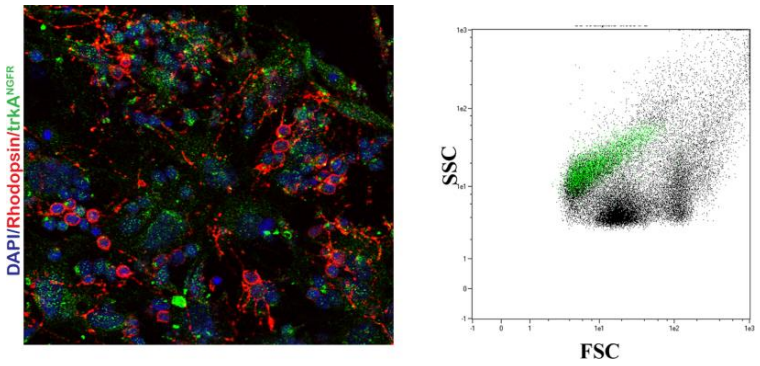

Figure 32
Immunofluorescence obtained by staining retinal photoreceptors of RCS mice with Rhodopsin and trkA^{NGFR} and a cytofluorometer plot of a retina single cell suspension gating the photoreceptors in green.

3.6 Conclusions

Reelin and NGF stand for two major signalling pathways alongside Central Nervous System (CNS) development and retinogenesis (**Levi-Montalcini 1987; D'Arcangelo et al. 1995**). The use of this second element, the solubilizing cap, permitted me to reconfirm, in an animal model of Autism, the reeler mouse, a significant increase of NGF and p75^{NTR} as well as unchanged trkA^{NGFR} levels in the Ganglion Cell Layer and in the Inner Nuclear Layer of *E-Reeler* retinas, as already shown in previous studies (**Balzamino et al. 2014**). Some protective NGF-p75^{NTR} effects were thereafter hypothesized, strongly supported by the observation that p75^{NTR} exerts both survival and apoptotic effects in developing CNS (**Nakamura et al. 2005; Balzamino et al. 2014**). To provide findings to support the hypothesis, RGCs, glial cells and RBCs were isolated from whole retinas and separated using a magnetic bead-coupled antibody procedure (**Angelucci et al. 2012**) and proteins

solubilized in the cap. Under physiological conditions, NGF and $p75^{NTR}$ were mainly expressed in all cell types, while $trkA^{NGFR}$ was weakly expressed by RBCs and RGCs, in line with literature (**Carmignoto et al. 1991; Shi et al. 2007**). As second point, low AnnexinV expression was detected in Reelin-deprived RGCs and RBCs. The high NGF and the low AnnexinV expressions in Reelin-deprived RGCs and RBCs might support the NGF protective effect. A NGF enriched microenvironment is consistent with a protective paracrine/autocrine effect played by endogenous NGF on RGCs and RBCs, as reported in other studies (**Siliprandi et al. 1993; Colafrancesco et al. 2011**). Cumulating, our findings suggest that during retina development NGF and $p75^{NTR}$ might contribute to protect E-Reeler RBCs and RGCs from degeneration, an attempt to preserve retinal circuit function. The possibility that other neurotrophins such as (BDNF, NT3, NT5), or angiogenic/angiostatic factors (VEGF/angiostatin), tissue enzymes (matrix Metalloproteinases) as well as soluble receptors (sTLRs and sTNFR) are involved in the process, should also be taken into consideration and remains to be addressed.

Photoreceptors of RCS rats expressed both $trkA^{NGFR}$ and $p75^{NTR}$ and were receptive to NGF exposure in both autocrine/paracrine manners, and several other *in vitro/in vivo* studies indicate that retinal cells produce, store and release biologically active NGF and express both $trkA^{NGFR}$/$p75^{NTR}$ receptors (**Micera A et al., 2004,2007**). Particularly, NGF promotes growth and survival of RGCs, either alone or in concert with other growth factors (**Siliprandi R et al., 1993**). The biochemical analysis confirmed the expression of $p75^{NTR}$ and as a new observation the expression of both inactive and phosphorylated $trkA^{NGFR}$ receptor forms. The Rhodopsin and $trkA^{NGFR}$ association suggests a critical protective link between NGF effect and photoreceptor survival, according to the well-known $trkA^{NGFR}$ properties (**Micera A et al., 2004**).

Several data from other models have highlighted the strong NGF ability to protect RGCs from degeneration (**Balzamino et al., 2015**; **Siliprandi R et al., 1993**). From this study, NGF administration might represent a critical survival factor not only

for RGC degeneration in Glaucoma and Maculopathy, but also for photoreceptor degeneration in RP.

As it outcomes from the data obtained with the use of the solubilizing cap, the results are comparable to those obtained with the traditional methods. Therefore, the use of this new device, will bring considerable benefits in terms of rapidity in obtaining good homogenized samples, that can be used directly for the research of specific biomarkers.

CHAPTER 4

Development of a Biosensor for Biomarker analysis

Abstract

The purpose of this thesis is to identify emerging biomarkers for eye diseases and to detect characteristic metabolites that can discriminate, with high specificity and high sensitivity the studied disease. Biosensor technologies, applied in clinically relevant situations, using integrated sampling devices strategies may deliver in real-time essential diagnostic data to patients or their treating clinicians, without the need of laboratory infrastructure. Proteomics research on body fluids distinguishes itself by the discovery of specific biomarkers for several diseases. The pursuit of biomarkers may be done conceiving a less invasive method to self-monitor the state of a disease, either through new biomarkers discovery for the development of new drugs and through the production of new devices. In this chapter, I will present the development of a biosensor made in collaboration with several laboratories of the CNR of the University of Tor Vergata. This biosensor will allow the electrochemically evaluation of one or more markers simultaneously. The design of this biosensor will enrich a patented device, composed of an ABS base in which the sensor will settle. Through another element explained in the previous chapter, the proteins solubilized from a previous sampling, will be drained on the sensor, which is spotted with a specific marker, and will emit an electrochemical signal giving an immediate response to the operator.

4.1 Background

Micro and nanofluidic are a very promising field of study and research in the biomedical field: micro or nano-tools can reveal both biological and chemical substances with higher sensitivity and responses faster than conventional systems. In addition, the ability to fabricate micro-sensors on chips paves the way for new types of on-board sensors, which are micro-sensors that can be analyzed

in-office and integrate data directly into a smartphone. Within this Ph.D., my intent was to use these emerging technologies to develop a handy, flexible, and sensitive protein-detecting device.

During my three years of Ph.D., my goal was to design and develop a new sampling and analysis devices to permit the research of specific biomarkers in ocular pathologies. For this reason, part of my Ph.D. was focused to understand some geometric and operational variables that will allow biological liquids to reach, by capillarity, an integrated chip on an analysis device through a private channel. In addition, a next step will be the development of a signal and data processing software, with the aim of making the most of the advantage offered by the time and reduced budget approach. The use of this device associated to the new chip, will contribute to the ophthalmology, enhancing the practicality and functionality of the sampling, and will exemplify through this software the interpretation of the data obtained.

The device will be made with inert material and functional for biological fluid withdrawals. It will be designed to be self-sufficient, and connected through a channel dedicated to a biomarker reading system (biosensor) for the biological fluid. You will then get a diagnostic system that will allow you to perform qualitative and quantitative biomarkers tests in real time. It can be produced in a kit, equipped with a data reader and a series of specific subsystems for different ocular pathologies, to be used in medical and outpatient clinics.

A second goal was to validate the device by analyzing different biomarkers in ocular pathologies. Initially, data were analyzed in the laboratory, with enzymatic assays present on the market, and then these assays were investigated directly on the device. The goal was to develop *ad-hoc* software and quantify in-office biomarkers, or to send data over radio frequencies to a reader such as a smartphone. From the analysis of literature, I selected IL6 as marker of ophthalmic pathologies with immunological and biochemical characteristics ideal for the realization of an electrochemical detection biosensor (**Jung JW et al., 2015; Irenaeus S et al., 2017; Chen Y et al., 2017**).

4.2 Characterization of the Biosensor Molecular Complex

My working aim was therefore to involve an electrochemical generation signal after the binding of the specimen sample on the chip visible in **Figure 33,** present in the socket of a patented device (ACkit), composed by a base in ABS with a membrane spotted with different targets, for the analysis of biomarkers present in a liquid sample, housed in an *ad hoc* socket, linked with a micro vessel to an injection hole, from which the biological fluid flows and deposits on the membrane (**Figure 33**). The new biosensor will take the place of the membrane and will have electrical connections that will allow to obtain an electrochemical result through the emission of signals picked up by a potentiostats.

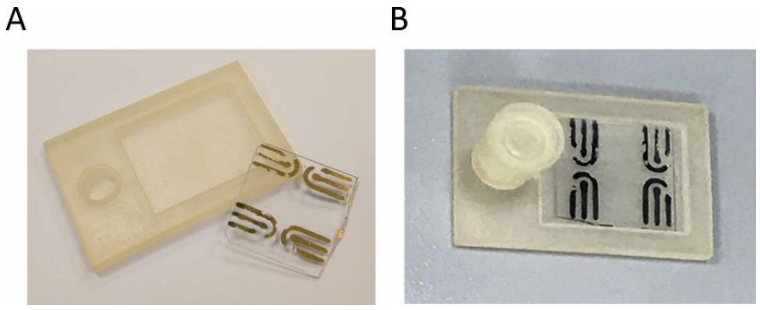

Figure 33
A Example of biosensor on glass chip and **B** ACkit assembled with biosensor and CAP.

In collaboration with the Institute of Translational Pharmacology (IFT), Institute of Microelectronics and Microsystems (IMM), Institute of Matter Structure (ISM) of the National Research Council (CNR), I have studied the structure of the biosensor, the protocols and the materials to be ordered.

In the first phase of study, I planned and carried out in collaboration with ISM, the experiments necessary for the deposition of a self-assembled monolayer (SAM) on a nanostructured wafer covered with gold. In the proposed biosensor, the SAM forms an intermediate molecular layer between the electrochemical sensor, the gold-plated nanophilic wafer (Au), and the antibody needed to recognize a molecular target (**Figure 34**). A blocking agent is used to avoid non-specific absorption on the surface. Gold is a material that has characteristics useful to

create a biosensor, it is inert enough not to be attacked by moisture or watery solutions, for this it can be exposed to humid conditions and used in a fluidic system. Furthermore, it has a specific reactivity in creating covalent bonds with specific molecules. To immobilize the antibodies on the golden surface, the biosensor has been incubated in ethanol solution, containing a self-embedded monolayer constituted by thiol groups, to bind the golden layer and carbossilic groups to bind the antibodies. To wash out the thiol groups in excess, not bind, washes were performed in HCl. At this point incubation was done in PBS with specific antibodies. After antibody incubation, another wash in ethanol is performed to remove the carbossilic group in excess not bind to the antibody. This step is fundamental to prevent non-specific binding during the detection steps.

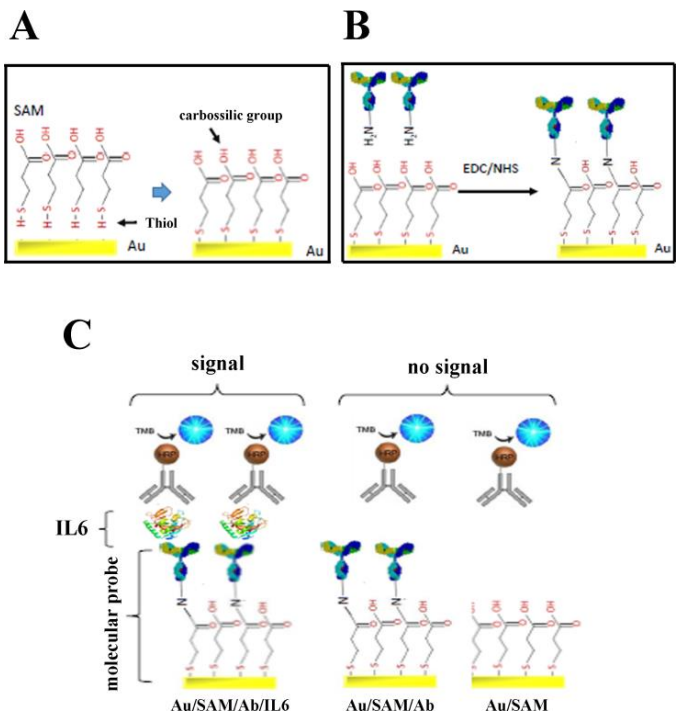

Figure 34
Development of a microchip in gold combined with the anti-IL6 for the detection of this interleukin involved in different eye pathologies.

To evaluate SAM deposition, X-ray photoelectron spectroscopy (XPS) measurements were performed to verify, characterize and determine the amount of SAM deposited on nanostructured wafer covered with gold. The XPS

measurements were carried out in collaboration with the ISM-CNR Material Institute, in each experiment my contribution was to provide the IL6 and verify its effective link with the SAM (**Figure 35**). The analysis of XPS data was done by ISM and the wafer used was made by the Institute of Microelectronics and Microsystems (IMM). As shown in **Figure 35,** in the first panel, the graph shows an electrochemical potential that is obtained from the protein-antibody bond at different concentrations, or a very low signal, if no protein binds the layer SAM-Antibody. While in the middle graph an absorbance result of the effective binding of the SAM to the antibody and to the gold is shown, only of the SAM to the gold or only the gold absorbance. These numeric results are also visible in the table on the right.

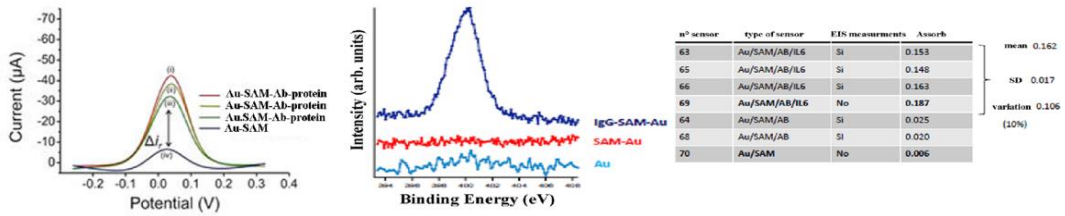

n° sensor	type of sensor	EIS measurments	Assorb
63	Au/SAM/AB/IL6	Si	0.153
65	Au/SAM/AB/IL6	Si	0.148
66	Au/SAM/AB/IL6	Si	0.163
69	Au/SAM/AB/IL6	No	0.187
64	Au/SAM/AB	Si	0.025
68	Au/SAM/AB	Si	0.020
70	Au/SAM	No	0.006

mean 0.162
SD 0.017
variation 0.106 (10%)

Figure 35
Electrochemical and Absorbance Measurements of the microchip embedded with the IL6 antibody.

Therefore, at the end of measurements in XPS, the experiments required to covalently bind the IL6 antibody to the probe, used as the initial model for prototype development were carried out. The molecular complex formed by Antibody-SAM-Au represents the molecular probe that, integrated on the measuring sensor, determines the molecular recognition of the target protein and mediates the electrochemical signal transduction (**Figure 34**). To accomplish the direct molecular probe against the IL6 target, I selected, based on the available scientific literature and available databases, an IL6 antibody that, by immunological characteristics, was specific to the IL6 target and that, by molecular structure and by chemical composition of the storage buffer, would be compatible with the antibody-binding protocol of the SAM (zero cross link) (**Qureshi A et al., 2010; Chikkaveeraiah BV et al., 2011**). I tested experimentally via ELISA the

binding of the antibody to the SAM-Au substrate as shown in **Figure 36**. To optimize the ELISA system, I experimentally determined the ideal reaction conditions. I determined secondary antibody concentrations, avidin-HRP concentrations, BSA concentration in the Blocking Solution, incubation times of the reagents and the number of washings to be carried out to reduce the background during the development of the test same. X-ray photoelectron spectroscopy (XPS) measurements were performed simultaneously to determine the presence of the antibody bound to the SAM-AU substrate.

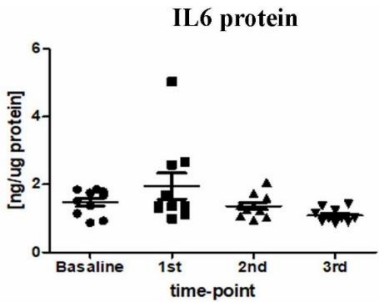

Figure 36
ELISA results of IL6 expression obtained with the complete layer formed by Au-SAM-Ab.

In the last phase of the biosensor development, in collaboration with the IMM and ISM Institutes, the experiments needed to characterize the electrochemical response of the biosensor in the presence and absence of disease markers for ophthalmic diseases. The electrochemical measurements were carried out by the IMM Institute using the Electrochemical Impedance Spectroscopy (EIS) technique (**Figure 35, first panel**).

During this experimental phase:

I realized the molecular probe, directed against the IL6 marker, on nanostructured gold sensors. Verified by ELISA and Simple Plex ELLA (**Figure 37**), the presence of the molecular probe under different conditions and at different times-points from the beginning of the experiment. The molecular probe was evaluated by ELISA and Simple plex ELLA, with control tears, to verify if the results obtained with the sensor in EIS, were similar with those of the actual laboratory techniques used to

evaluate the quantity of a specific protein. These tests were used to evaluate the integrity of the molecular probe over time, chemical storage buffer storage, and biosensor storage temperatures. And at last I verified by ELISA the presence of IL6 linked to the molecular probe to validate the response of the biosensor made for the ELISA test, and therefore, useful to detect disease markers in biological samples.

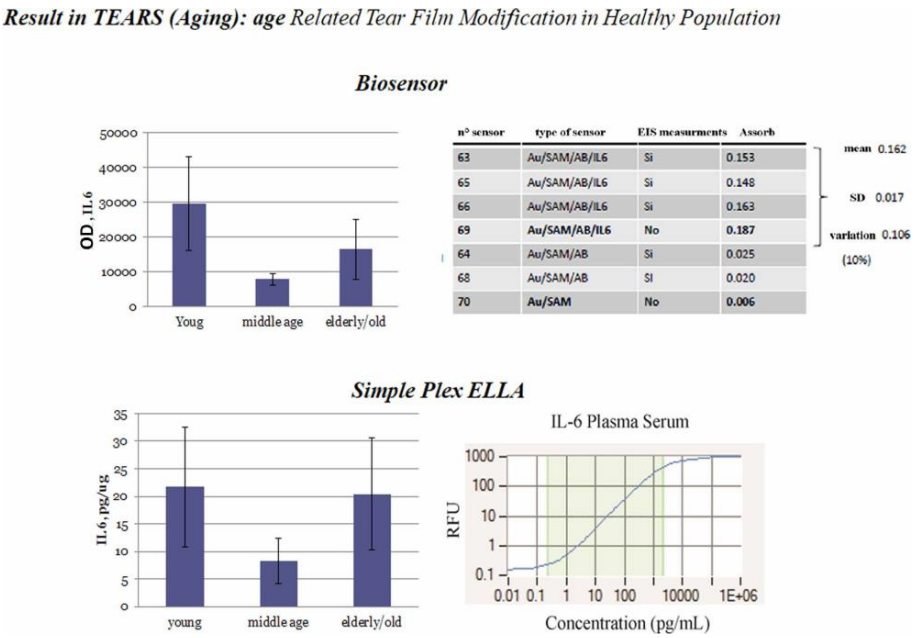

Figure 37
Laboratory Experimental validation of the complex Au-SAM-antibody.

This has been possible, evaluating the concentration, chemical formulation and buffer pH used during Amperometric measurements to obtain the best relationship between molecular probe stability, probe interaction stability with biomarker and electrochemical response of the sensor. In particular, the proposed biosensor is an electrochemical biosensor composed of three electrodes: Working Electrode (WE), Counter Electrode (CE) and Reference Electrode (RE). **Figure 38** shows an image of the biosensor realized, highlighting the geometry and the materials constituting the electrodes.

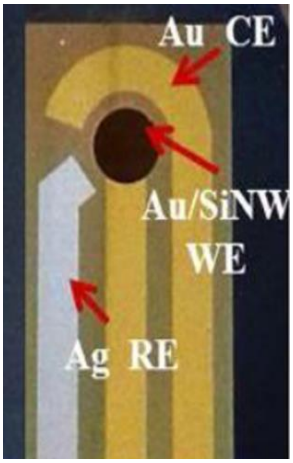

Figure 38
Electrochemical biosensor device. Geometry of the electrodes constituting the electrochemical biosensor.

The WE, which represents the sensitive part of the transducer or the surface on which the reaction of interest takes place, consists of silicon nanowires coated with gold (Au / Silicon NanoWires, Au / SiNW). I opted together with the IMM and ISM for a nanostructured material, because it has many advantages: it is a porous structure easily accessible to gases or liquids containing biological analytes and the presence of the nanowires involves a considerable increase of the interaction surface for the biomolecules, compared to a gold surface. The WE was then functionalized to link the cytokine (IL6) present in tears. Defined the process steps necessary for the realization of the device, the electrode was obtained from a 3-inch silicon (wafer) substrate with a layer of 1 µm oxidized. The phases to obtain a WE are here reported:

* Initial phase substrate cleaning.

* WE lithographic process with UV exposure.

* Evaporation of a thin layer of gold (4-5 nm) which acts as a catalyst for the growth of nanowires;

* Growth of silicon nanowires by plasma enhanced chemical vapor deposition, through VLS (Vapor Liquid Solid) mechanism.

Each lithography is followed by an evaporation process through which there is a coating of the electrodes with metal films. In particular, the RE is made of Ag (thickness of 100 nm) while the CE and WE in gold (thickness of 150 nm), as shown in **Figure 38**. Once the three electrodes are obtained, the passivation of the device is carried out through a layer of Polyimide (PI), deposited by a spin-coating process on the entire wafer.

Once the process steps have been fine-tuned, in collaboration with the IFT, we focused on the possibility of increasing the density of the WE nanowires according to the degree of cleaning of the substrate, so as to further increase the binding surface for the biomolecules of our interest present in tears. The results of this and other optimization studies of the device manufacturing process will be my future goals.

4.3 Results

4.3.1 Optimization of Experimental Parameters

To obtain the best analytical performance, optimization of the experimental conditions was performed. The pH played a pivotal role in the preparation of the conjugate. The highest assay sensitivity was reached if pH 5.0 was used as shown in **Figure 39A**. A relationship was obtained between the anode potential and pH, suggesting the participation of protons during the electrochemical process. A good pH is, consequently, an optimal set-up point, that ensures the highest level of gold surface coverage by the antibody. Another important factor is the time of exposure of the SAM and Ab for the response signal.

Incubation time is important for the analytical performance of the immunoassays, therefore we obtained a constant value after an incubation time of 50 min, showing a good binding between the sample and the antibodies. Hence, 50 min of incubation was selected for binding condition as visible in the right graph of **Figure 39B**. We developed a standard calibration curve for different biomarkers detection.

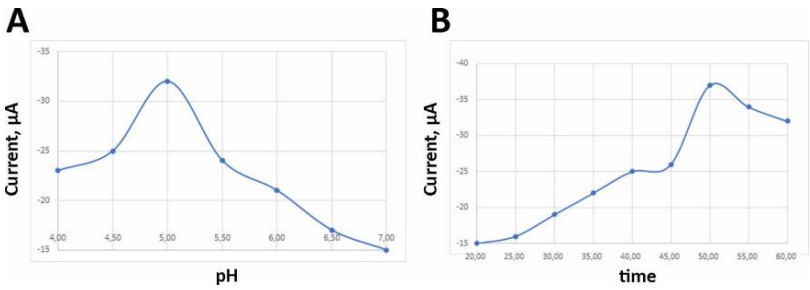

Figure 39
Graphs of pH and time related to the current obtained during tests of the biosensors.

This pH 5.0 is therefore, optimal for conjugation, warranting a high level of gold surface coverage by the antibody. Incubation time of 50min with the complex is the best parameter affecting the analytical performance of the immunoassays, which was carried out using the described electrochemical conditions.

4.3.2 Comparison of Electrochemical Responses

One main advantage in using customized chips is the possibility to control and adapt their properties to meet the needs of a single biomarker or a panel of markers (**Yang Z. et al, 2012**). The standard solutions were analyzed and compared to the results obtained with the new biosensor, using common laboratory assays like, the ELISA procedure. The signals obtained were recorded, resulting more sensitive with respect to the ELISA assay. These results indicated that using the chip instead of old laboratory assays enhanced the sensitivity of the signal and therefore the output response is more reliable. We believe that this result demonstrates that a good device act successfully for clinical diagnosis in short time.

A further result obtained on the IL6, using the biosensor, is the measure of the variation in percentage shown in table below:

• On the 0.1 Hz impedance module: $\Delta \mid Z \mid = 37\%$

• On the Z phase at 0.1 Hz: $\Delta\Phi = 35\%$

Biosensor output to IL6		
N° samples	**Δ $IZI_{0.1\%\ Hz}$ %**	**Δ $\phi_{0.1\%\ Hz}$ %**
1	21%	16%
2	39%	43%
3	22%	19%
4	50%	54%
5	57%	41%

4.5 Discussion

4.5.1 Preliminary tests for Selectivity and Repeatability

An important selection of different biomarkers plays a main role in analyzing biological samples. To investigate the specificity of the biosensor, we tested the system with different biomarkers including IL6 and NGF. As shown in **Figure 35**, preliminary tests were performed, and the biosensor showed a stable signal with the Au particles only. On the contrary, low current responses were exhibited by the markers used. These results indicated a good specificity.
Furthermore, the assay was investigated with intra- and inter-assay experiments. These results demonstrated that the device possessed an adequate reproducibility (**Figure 26-28,36,37**).

Finally, as a last resort, it is expected to be applied in hospital districts, more precisely in the surgical/preambulatory and ophthalmological field. This device can be used to evaluate prognostic markers of drug therapy. The active part of the chip will consist of the biomarker, a protein traceable in the biological fluid and representative of a pathological condition, an indispensable indicator for the physician who decides on a diagnostic question. Operation and sensitivity of the device was validated by calibration and use in ambulatory and / or chirurgic practice.

4.5.2 Future Perspective

To standardize the lectures and the outcome of the potentiostats, a commercial approach was selected, these microchips are available on DropSense website (www.dropsens.com/en/screen_printed_electrodes_pag.html). These disposable Electrodes are aimed at detecting eight signals simultaneously, allowing (differential) measurement of up to eight analytes in the solution. They are suitable for working with microvolumes, typically 1-3µL, for decentralized assays or to develop specific (bio)sensors. Specially designed for the development of multiple simultaneous analysis.

Ceramic substrate: L50 x W27 x H1 mm

Electric contacts: Silver

The electrochemical cell consists of:

8 Working electrodes: Carbon (2.95mm diameter)

Auxiliary electrode: Carbon

Reference electrode: Silver

This electrode is recommended to be used with a µStat Multi Potentiostat/Galvanostat. The working electrodes are made of carbon, like the counter electrode and a silver reference electrode. They are aimed at detecting signals simultaneously, allowing (differential) measurement of analytes in the solution (**Figure 40**).

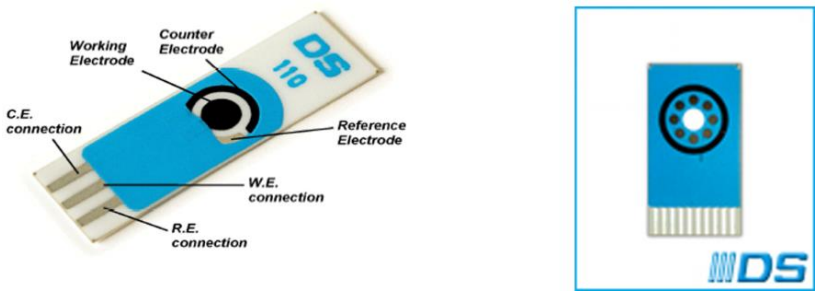

Figure 40
DropSense chips. On the left a one marker chip and on the right a multiple marker sensor.

To allow the insertion of this microchip purchased on DropSense web site, in the patented device described in the chapter above, thanks to Solidworks, the chamber, prepared for the housing of the nitrocellulose membrane, of the ACkit device, has been reduced and permits the perfect housing of a customized DropSense microchip. The upper opening has been closed (**Figure 41AB**) and leaved only a hole to permit the loading of the sample on the chip (**Figure 41C**).

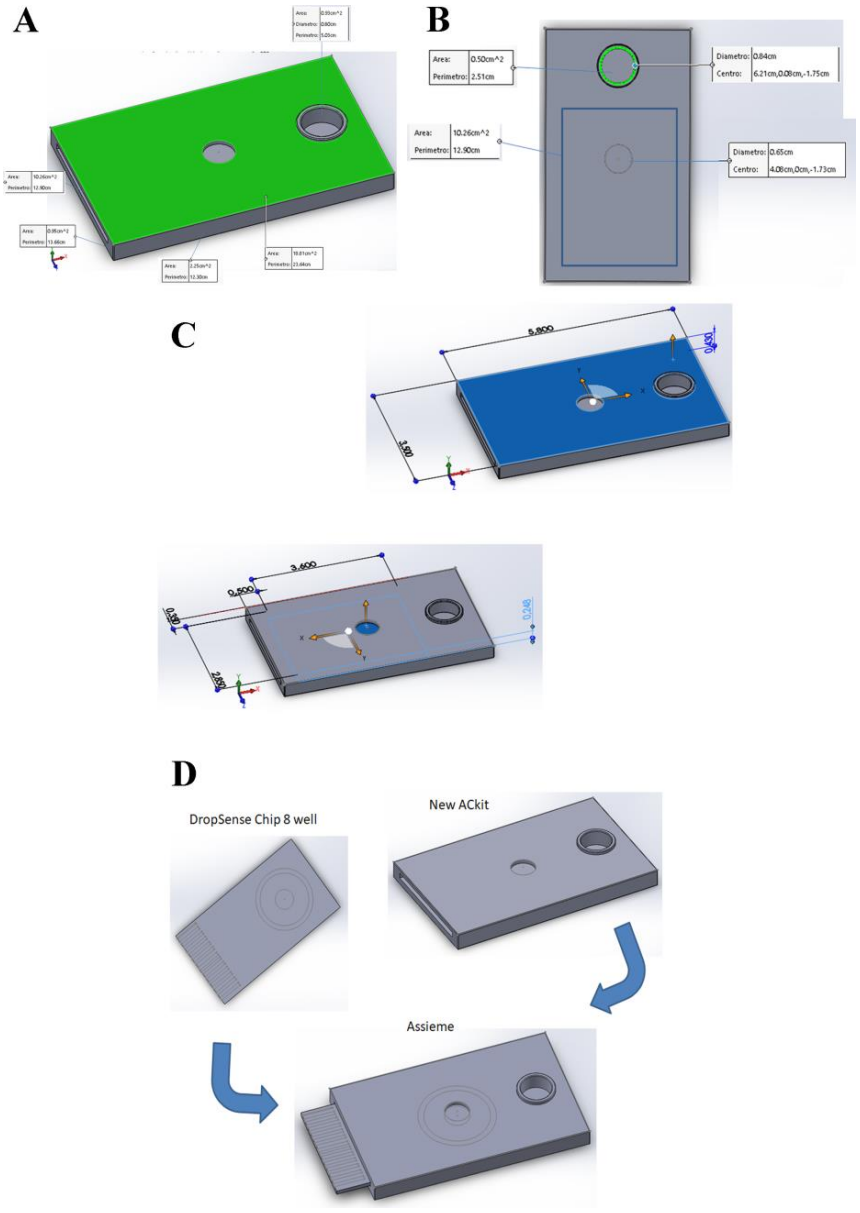

Figure 41
Evolution of the ACkit patented device in ACkit 3.0, with the incorporation of a DropSense microchip.

CHAPTER 5

Conclusions

5.1 Ensuring the availability of safe and effective diagnostics

The success of the personalized medicines is determined by the identification of biomarkers and the successful development of diagnostic devices. Scientific discoveries brought a high percentage of biological information, while the development of diagnostics devices and the translation into clinical practice pose various challenges. Inadequate diagnostic tests can have severe therapeutic consequences (**Ventola CL, 2011**).

5.2 Potential relapse

Eye disorders are extremely widespread and characterized by various grades of symptoms, with high impact on quality of life and high socio-economic costs. Therefore, the study of the involvement of new biomarkers, through molecular studies, proteomics, gene silencing and translation of the intracellular signal, would contribute to increase the knowledge of the pathophysiological mechanisms underlying ocular pathologies. The aim of my Ph.D. was the research of specific biomarkers of ocular diseases. Therefore, the design and development of new sampling devices, or analyzing devices, permits the pursuit of markers involved in different pathologies. The results of this study will favor the development of new therapeutic approaches and/or diagnostic strategies to apply to the eye.

These devices, will provide a very rapid initial diagnosis in medical care (specialist and non-medical) and reduce healthcare times/costs, partly reducing SSN through addressing specialist centers. The ability to select different combinations of biomarkers will allow the device to be used in other strategic areas of great health, environmental and commercial interest (Veterinary, Cosmetics and Agro-Food). In Ophthalmology, there is strong interest in portable

diagnostic support devices, this can provide diagnosis/prognosis information, significantly reducing the waiting time of a report, typically ranging from 1 to 2 weeks.

My intent was to create a useful device for the specialist to undertake an in-office diagnosis without resorting to sophisticated and advanced instrumentation present only in large structures or centers of excellence. At the same time, the device would provide added value in multicenter national/international studies, allowing an analysis of operational units by sending the coordinator center of the information collected in 2-3 hours through databases, thus avoiding the shipment of biological material. The device will be equipped with chips to detect different pathologies, readout support, and differential diagnosis guidelines (validation with the help of specialized medical personnel).

Therefore, its use will allow you to make all the steps of the operating procedure at any place outside a research laboratory (outpatient clinic, private or public study, consultants, ASL, non-sanitary sampling sites). From the point of view of the originality of acquiring knowledge, it should be noted that part of the Ph.D. activity has been devoted to the study of the design and functionalization of the sensor that interacts with the biomarkers. The results gained in part and otherwise will be published in international scientific journals and will thus contribute to the enhancement of knowledge of science-related topics of great public interest.

The use of this device would allow the use of proven data to validate lab research, or for instance to conduct opinion mining between distant locations. By utilizing past knowledge and new data, you could make a bigger learning on a huge amount of data that a biologist can hardly handle by hand, and the biologist himself might have ideas for new search directions. In addition, the new knowledge learned would be used to update existing knowledge. The total cost for each chip is very low, this provides a cheaper alternative to the current *in vitro* studies. Obviously, if successful, the benefits of the device would be very substantial.

5.3 Conclusions and future developments

As shown in the second chapter, impression cytology is a technique that allows rapid and painless sampling of ocular (conjunctival and corneal) surface layers for biomolecular analysis to support bio-instrumental outpatient investigation. The methodology could be an alternative method to biopsy (in some pathologies) and is applied to experimental diagnosis and clinical trials.

The analysis of the requirements previously carried out revealed many features and criticalities that the devices currently on the market do not fill. Therefore, during my Ph.D. I designed a device that improves current sampling techniques, essentially based on the manual skills of the specialist physician. Therefore, the device, object of this study, seeks to improve both the sampling method and its effectiveness by intervening on the positioning method of the sample instrument on the eye surface using the nitrocellulose membrane.

The main intention was to create a device that can integrate the nitrocellulose membrane already present on the market and currently used for impression cytology (Millicell) and allow a simple and convenient sampling. Thus, an extremely simple and repeatable, non-painful, non-invasive and effective method was developed, enabling a sampling procedure that allows unlimited use of cytodiagnostic techniques in different areas, both medical and non-medical.
The device and its method of utilization allow the development of a highly tolerated sampling that leads to an improvement in the level of accuracy and repeatability of the technique, as previously demonstrated by analysis performed on samples taken on three volunteers, and after having analyzed the cellular populations present using different methods. According to the evaluation questionnaires submitted to operators that perform cytological sampling for specific diagnostics or Clinical Trials, the device resulted lightweight, flexible and ergonomic, increasing the precision level. The device reduces the intervention time and facilitates the sampling procedure both on the operator side and on the patient side. The use of the device is highly flexible as the membranes offer different possibilities of histological, biochemical and molecular analysis to support bio-instrumental outpatient analysis. Thus, biomarkers can predict both

the typology and size of tissue damage, allowing rapid evaluation (diagnosis/prognosis in medicine and veterinarian). Rapid response is a very useful requirement especially in the field of ophthalmic surgery, where damage can result in a subsequent corneal lesion. Histological analysis carried out on a larger population sample will enable the device to be better valued and calibrated before being placed on the market.

A link between the new sampling device and the new biosensor integrated with the patented device, is the CAP. Thanks to its utility, for biological samples, through an extraction solution, protein contained in the samples, will be extracted and returned in liquid form. Subsequently, the sample is pulled through a micro channel on the analysis device, on to a membrane spotted with different biomarkers or like in our case, on to a customized microchip spotted with specific disease markers. The use of this cap, will reduce time and operator errors in the extraction procedures and the marking steps.

A further activity carried out during my Ph.D. has been the development in collaboration with the CNR of the University of Tor Vergata, of a biosensor characterized by a specific link with a specific marker correlated to an ocular pathology, the production of an electrochemical sensors chips, offers important features, low cost of production, easy to use methods, and small sample need. Their sensitivity and selectivity are correlated directly to the nanomaterials employed in their construction (**Farghali RA et al., 2015**). A single bare gold electrode was used to generate distinctive electrochemical signatures for a specific biomarker, IL6, linked to different eye disorders. The main advantages of this approach include portability thanks to its miniaturization, rapid detection, reliable and inexpensive way, which enhances screening applications. Future studies will be needed for the development of this sensors, conjugating a good software for the result lecture. The use of the device will contribute not only to ophthalmology, but also to improving reproducibility and sampling functionality, and will simplify the interpretation of the data obtained through this software.

The need to have sampling devices that are small, manageable and functional, is based on my own field of expertise in the field of ophthalmology, in which one works in a system such as the eye, which leads to a small amount of material to work on it.

In conclusion, my contribution was both biomolecular and biochemical, enabling the integration of engineering and physical knowledge with those in the biomedical field. As visible in the scheme below, I tried to represent, for my PhD, a link for all my aims, in order to obtain from a sampling, directly, a specific biomarker solubilized in the CAP and analyzed with the biosensor.

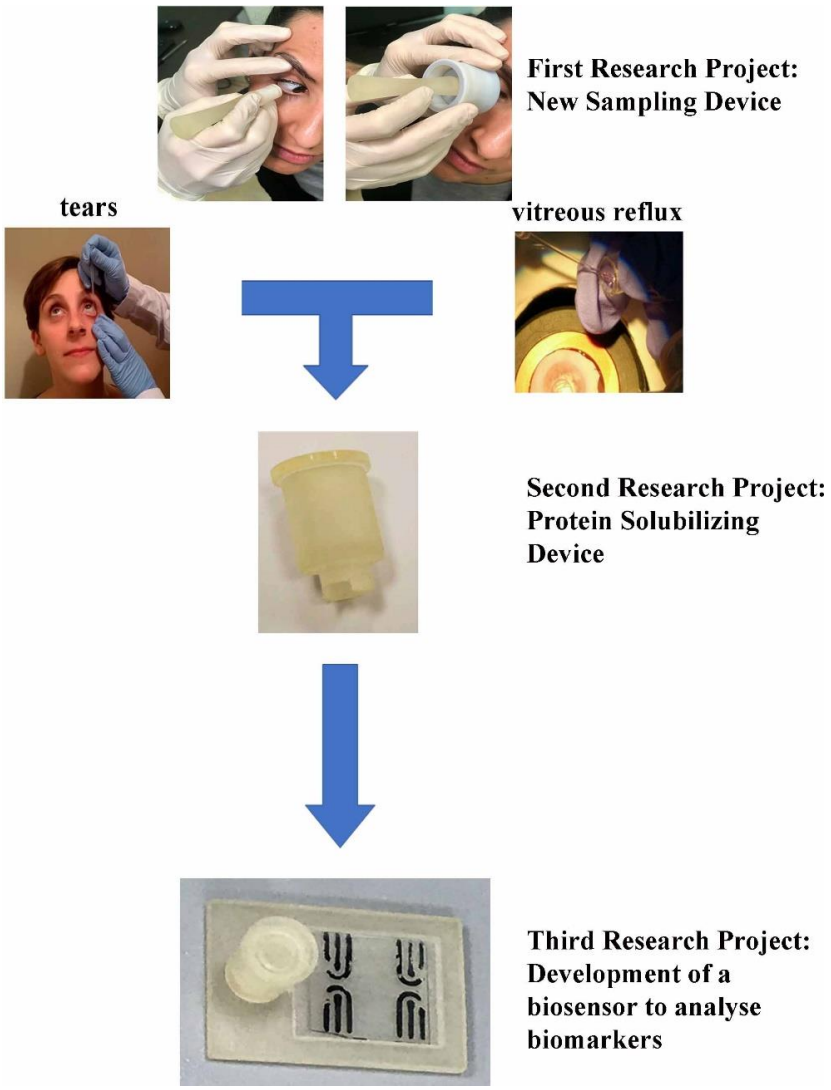

Scheme 2
Diagram illustrating the different projects addressed in these three years of Ph.D.

LIST OF PUBLICATION

International workshops and national conferences

Bijorn Omar Balzamino, Graziana Esposito, Ramona Marino, Flavio Keller, Alessandra Micera. Biochemical analysis of vitreous from Reelin deficient mice: NGF and VEGF study. THE FIRST INTERNATIONAL RITA LEVI-MONTALCINI'S SCIENTIFIC MEETING NERVE GROWTH FACTOR: NEUROSCIENCE AND THERAPY. Bologna, Italy.

Bijorn Omar Balzamino, Loredana Zollo, Alessandra Micera. Dispositivi per campionamento superficie oculare: progettazione e realizzazione. Workshop MaBIOS. Rome, Italy.

International journal publications

Submitted

Research Paper

Aloe L, Rocco ML, **Balzamino BO**, Micera A. Purified retrobulbar anti-ngf antibodies administration induces structural and biochemical alteration in the corneal and retinal cells. Clinical & Experimental Ophthalmology

Published

Research Paper

Rocco ML, **Balzamino BO**, Aloe L, Micera A. NGF protects corneal, retinal and cutaneous tissues/cells from phototoxic effect of uv exposure. Graefes Arch Clin Exp Ophthalmol. 2018 Apr;256(4):729-738. doi: 10.1007/s00417-018-3931-y. Epub 2018 Feb 15. PMID: 29450621

Research Paper

Rocco ML, **Balzamino BO**, Esposito G, Petrella C, Aloe L, Micera A. NGF/anti-VEGF combined exposure protects RCS retinal cells and photoreceptors that underwent a local worsening of inflammation. Graefes Arch Clin Exp Ophthalmol. 2017 Mar;255(3):567-574. doi: 10.1007/s00417-016-3567-8. Epub 2016 Dec 24. PMID: 28013393

Review Paper

Micera A, **Balzamino BO**, Biamonte F, Esposito G, Marino R, Fanelli F, Keller F. Current progress of Reelin in development, inflammation and tissue remodeling: from nervous to visual systems. Curr Mol Med. 2016 Aug 5. PMID: 27494703

Review Paper

Aloe L, Rocco ML**, Balzamino BO**, Micera A. Nerve growth factor: role in growth, differentiation and controlling cancer cell development. J Exp Clin Cancer Res. 2016 Jul 21;35(1):116. doi: 10.1186/s13046-016-0395-y. PMID: 27439311

Review Paper

Micera A, **Balzamino BO**, Di Zazzo A, Biamonte F, Sica G, Bonini S. Toll-Like Receptors and Tissue Remodeling: The Pro/Cons Recent Findings. J Cell Physiol. 2016 Mar;231(3):531-44. doi: 0.1002/jcp.25124. Epub 2015 Sep 1. PMID: 26248215

Review Paper

Aloe L, Rocco ML, **Balzamino BO**, Micera A. Nerve Growth Factor: A Focus on Neuroscience and Therapy. Curr Neuropharmacol. 2015;13(3):294-303. PMID: 26411962

Research Paper

Balzamino BO, Esposito G, Marino R, Keller F, Micera A. NGF Expression in Reelin-Deprived Retinal Cells: A Potential Neuroprotective Effect. Neuromolecular Med. 2015 Sep;17(3):314-25. doi: 10.1007/s12017-015-8360-z. PMID: 26066836

Research Paper

Rocco ML, **Balzamino BO**, Petrocchi Passeri P, Micera A, Aloe L. Effect of purified murine NGF on isolated photoreceptors of a rodent developing retinitis pigmentosa. PLoS One. 2015 Apr 21;10(4):e0124810. doi: 10.1371/journal.pone.0124810. PMID: 25897972

Patent

Sampling device of the ocular surface by imprinting. SurfAL" inventors: MICERA Alessandra, ZOLLO Loredana, **BALZAMINO Bijorn Omar**, GHEZZI Ilaria, SGRULLETTA Roberto (PCT/IB2016/051474; 04/2016)

Grant Regione Lazio: Researcher in support in MaBIOS Research Project (LR13/2008) Matrici di biosensori a trasduzione elettrica su pellicole polimeriche per kit diagnostici e monitoraggio terapeutico di malattie oftalmiche (FILAS-RU-2014-112)

BIBLIOGRAPHY

Aloe L, Rocco ML, Balzamino BO, Micera A. Nerve Growth Factor: A Focus on Neuroscience and Therapy. Curr Neuropharmacol. 2015;13(3):294-303. Review. PMID:26411962

Aloe L, Rocco ML, Balzamino BO, Micera A. Nerve growth factor: role in growth, differentiation and controlling cancer cell development. J Exp Clin Cancer Res. 2016 Jul 21;35(1):116. doi: 10.1186/s13046-016-0395-y. Review. PMID:27439311

Alomar MJ. Factors affecting the development of adverse drug reactions (Review article). Saudi Pharm J. 2014 Apr;22(2):83-94. doi: 10.1016/j.jsps.2013.02.003. Epub 2013 Feb 24.

Angelucci C, Maulucci G, Lama G, Proietti G, Colabianchi A, Papi M, Maiorana A, De Spirito M, Micera A, Balzamino OB, Di Leone A, Masetti R, Sica G. Epithelial-stromal interactions in human breast cancer: effects on adhesion, plasma membrane fluidity and migration speed and directness. PLoS One. 2012;7(12):e50804. doi: 10.1371/journal.pone.0050804. Epub 2012 Dec 10. PMID:23251387 PMCID:PMC3519494 DOI:10.1371/journal.pone.0050804

Aronni S, Cortes M, Sacchetti M, Lambiase A, Micera A, Sgrulletta R, Bonini S. Upregulation of ICAM-1 expression in the conjunctiva of patients with chronic graft-versus-host disease. Eur J Ophthalmol. 2006 Jan-Feb;16(1):17-23.

Balzamino BO, Esposito G, Marino R, Keller F, Micera A. NGF Expression in Reelin-Deprived Retinal Cells: A Potential Neuroprotective Effect. Neuromolecular Med. 2015 Sep;17(3):314-25. doi: 10.1007/s12017-015-8360-z. Epub 2015 Jun 12. PMID:26066836

Bekerman I, Gottlieb P, Vaiman M. Variations in eyeball diameters of the healthy adults. J Ophthalmol. 2014;2014:503645. doi: 10.1155/2014/503645. Epub 2014 Nov 5.

Bell KA, Kobayashi I, Chen Y, Mellman TA. Nocturnal autonomic nervous system activity and morning proinflammatory cytokines in young adult African Americans. J Sleep Res. 2017 Aug;26(4):510-515. doi: 10.1111/jsr.12480. Epub 2017 Feb 17. PMID:28211138

Burd EM. Validation of laboratory-developed molecular assays for infectious diseases. Clin Microbiol Rev. 2010 Jul;23(3):550-76. doi: 10.1128/CMR.00074-09. Review. PMID:20610823

Cacciamani A, Parravano M, Scarinci F, Esposito G, Varano M, Micera A. A Simple Spontaneous Vitreal Reflux Collecting Procedure During Intravitreal Injection: Set-Up and Validation Studies. Curr Eye Res. 2016 Jul;41(7):971-6. doi: 10.3109/02713683.2015.1080282. Epub 2015 Oct 15. PMID:26470652

Carmignoto G, Comelli MC, Candeo P, Cavicchioli L, Yan Q, Merighi A, Maffei L. Expression of NGF receptor and NGF receptor mRNA in the developing and adult rat retina. Exp Neurol. 1991 Mar;111(3):302-11.

Chikkaveeraiah BV, Mani V, Patel V, Gutkind JS, Rusling JF. Microfluidic electrochemical immunoarray for ultrasensitive detection of two cancer biomarker proteins in serum. Biosens Bioelectron. 2011 Jul 15;26(11):4477-83. doi: 10.1016/j.bios.2011.05.005. Epub 2011 May 11. PMID:21632234

Choy C, Benzie I, Cho P. Antioxidants in tears and plasma: Inter-relationships and effect of vitamin C supplementation. Curr Eye Res. 2003 Jul;27(1):55-60. PMID:12868009

Church D, Kerr R, Domingo E, Rosmarin D, Palles C, Maskell K, Tomlinson I, Kerr D (2014). "Toxgnostics': an unmet need in cancer medicine". Nat Rev Cancer (6):440-5

Coassin M, Lambiase A, Sposato V, Micera A, Bonini S, Aloe L. Retinal p75 and bax overexpression is associated with retinal ganglion cells apoptosis in a rat model of glaucoma. Graefes Arch Clin Exp Ophthalmol. 2008 Dec;246(12):1743-9. doi: 10.1007/s00417-008-0913-5. Epub 2008 Aug 27. PMID:18751719

Cohen JP, Felix AE. Personalized Medicine's Bottleneck: Diagnostic Test Evidence and Reimbursement. J Pers Med. 2014 Apr 4;4(2):163-75. doi: 10.3390/jpm4020163. PMID:25563222

Colafrancesco V, Coassin M, Rossi S, Aloe L. Effect of eye NGF administration on two animal models of retinal ganglion cells degeneration. Ann Ist Super Sanita. 2011;47(3):284-9. doi: 10.4415/ANN_11_03_08.

D'Arcangelo G, Miao GG, Chen SC, Soares HD, Morgan JI, Curran T. A protein related to extracellular matrix proteins deleted in the mouse mutant reeler. Nature. 1995 Apr 20;374(6524):719-23. PMID:7715726

Dartt DA, Masli S. Conjunctival epithelial and goblet cell function in chronic inflammation and ocular allergic inflammation. Curr Opin Allergy Clin Immunol. 2014 Oct;14(5):464-70. doi: 0.1097/ACI.0000000000000098.

Differential Protein Expression Profiles in Glaucomatous Trabecular Meshwork: An Evaluation Study on a Small Primary Open Angle Glaucoma Population. Adv Ther. 2016 Feb;33(2):252-67. doi: 10.1007/s12325-016-0285-x. Epub 2016 Jan 28. PMID:26820987

Dingel MJ, OstergrenJ, McCormick JB, Hammer R, Koenig BA. (2015). "The media and behavioral genetics: Alternatives coexisting with addiction genetics". Sci Technol Human Values. 2015 Jul 1; 40(4): 459–486. doi:10.1177/0162243914558491 PMCID: PMC4574304

Egbert PR, Lauber S, Maurice DM. A simple conjunctival biopsy. Am J Ophthalmol. 1977 Dec;84(6):798-801. PMID:596392

Egnew and Thomas E. (2009). "Suffering, Meaning, and Healing: Challenges of Contemporary Medicine". Annals of Family Medicine. 7 (2): 170–175. doi:10.1370/afm.943. Retrieved 6 January 2016.

Elder MJ, Dart JK, Lightman S. Conjunctival fibrosis in ocular cicatricial pemphigoid--the role of cytokines. Exp Eye Res. 1997 Aug;65(2):165-76. PMID:9268585

Eördögh R, Schwendenwein I, Tichy A, Nell B. Impression cytology: a novel sampling technique for conjunctival cytology of the feline eye. Vet Ophthalmol. 2015 Jul;18(4):276-84. doi: 10.1111/vop.12244. Epub 2014 Dec 29. PMID:25557393

Farghali RA, Fekry AM, Ahmed RA, Elhakim HK. Corrosion resistance of Ti modified by chitosan-gold nanoparticles for orthopedic implantation. Int J Biol Macromol. 2015 Aug;79:787-99. doi: 10.1016/j.ijbiomac.2015.04.078. Epub 2015 May 16. PMID:25989146

Gulley ML, Shea TC, Fedoriw Y. Genetic tests to evaluate prognosis and predict therapeutic response in acute myeloid leukemia. J Mol Diagn. 2010 Jan;12(1):3-16. doi: 10.2353/jmoldx.2010.090054. Epub 2009 Dec 3. Review. PMID:19959801

Irenaeus S, Schiza A, Mangsbo SM, Wenthe J, Eriksson E, Krause J, Sundin A, Ahlström H, Tötterman TH, Loskog A, Ullenhag GJ. Local irradiation does not enhance the effect of immunostimulatory AdCD40L gene therapy combined with low dose cyclophosphamide in melanoma patients. Oncotarget. 2017 Jul 31;8(45):78573-78587. doi: 10.18632/oncotarget.19750. eCollection 2017 Oct 3. PMID:29108250

Irkeç M, Bozkurt B. Epithelial cells in ocular allergy. Curr Allergy Asthma Rep. 2003 Jul;3(4):352-7. Review. PMID:12791215

Journée-de Korver HG, Midena E, Singh AD. Infrared thermotherapy: from laboratory to clinic. Ophthalmol Clin North Am. 2005 Mar;18(1):99-110, viii-ix. PMID:15763195 DOI:10.1016/j.ohc.2004.08.008

Jung JW, Han SJ, Song MK, Kim TI, Kim EK, Min YH, Cheong JW, Seo KY. Tear Cytokines as Biomarkers for Chronic Graft-versus-Host Disease. Biol Blood Marrow

Transplant. 2015 Dec;21(12):2079-2085. doi:10.1016/j.bbmt.2015.08.020. Epub 2015 Aug 22. PMID:26303101 DOI:10.1016/j.bbmt.2015.08.020

Kim YS, Jo DH, Lee H, Kim JH, Kim KW, Kim JH. Nerve growth factor-mediated vascular endothelial growth factor expression of astrocyte in retinal vascular development. Biochem Biophys Res Commun. 2013 Feb 22;431(4):740-5. doi: 10.1016/j.bbrc.2013.01.045. Epub PMID:23337506 DOI:10.1016/j.bbrc.2013.01.045

Kurpakus MA, Maniaci MT, Esco M. Expression of keratins K12, K4 and K14 during development of ocular surface epithelium. Curr Eye Res. 1994 Nov;13(11):805-14. PMID:7531631

Lai TL, Lavori PW, Shih MC, Sikic BI. Clinical trial designs for testing biomarker-based personalized therapies. Clin Trials. 2012 Apr;9(2):141-54. doi: 10.1177/1740774512437252. Epub 2012 Mar 7. PMID:22397801

Lambiase A, Merlo D, Mollinari C, Bonini P, Rinaldi AM, D' Amato M, Micera A, Coassin M, Rama P, Bonini S, Garaci E. Molecular basis for keratoconus: lack of TrkA expression and its transcriptional repression by Sp3. Proc Natl Acad Sci U S A. 2005 Nov 15;102(46):16795-800. Epub 2005 Nov 7. PMID:16275928

Lambiase A, Coassin M, Costa N, Lauretti P, Micera A, Ghinelli E, Aloe L, Rama P, Bonini S. Topical treatment with nerve growth factor in an animal model of herpetic keratitis. Graefes Arch Clin Exp Ophthalmol. 2008 Jan;246(1):121-7. Epub 2007 May 4. PMID:17479276

Levi-Montalcini R. The nerve growth factor 35 years later. Science. 1987 Sep 4;237(4819):1154-62. Review. No abstract available. PMID: 3306916

Lin H, Yiu SC. Dry eye disease: A review of diagnostic approaches and treatments. Saudi J Ophthalmol. 2014 Jul;28(3):173-81. doi: 10.1016/j.sjopt.2014.06.002. Epub 2014 Jun 24. PMID:25278793

Marko CK, Tisdale AS, Spurr-Michaud S, Evans C, Gipson IK. The ocular surface phenotype of Muc5ac and Muc5b null mice. Invest Ophthalmol Vis Sci. 2014 Jan 15;55(1):291-300. doi: 10.1167/iovs.13-13194.

Marton MJ and Weiner R. Practical Guidance for Implementing Predictive Biomarkers into Early Phase Clinical Studies. Biomed Res Int. 2013; 2013: 891391. doi: 10.1155/2013/891391.

McCaa CS. The eye and visual nervous system: anatomy, physiology and toxicology. Environ Health Perspect. 1982 Apr;44:1-8. PMID:7084144

Micera A, Balzamino BO, Biamonte F, Esposito G, Marino R, Fanelli F, Keller F. Current progress of Reelin in development, inflammation and tissue remodeling: from nervous to visual systems. Curr Mol Med. 2016 Aug 5. PMID:27494703

Micera A, Di Zazzo A, Esposito G, Sgrulletta R, Calder VL, Bonini S. Quiescent and Active Tear Protein Profiles to Predict Vernal Keratoconjunctivitis Reactivation. Biomed Res Int. 2016;2016:9672082. doi: 10.1155/2016/9672082. Epub 2016 Feb 17. PMID:26989694

Micera A, Lambiase A, Aloe L, Bonini S, Levi-Schaffer F, Bonini S. Nerve growth factor involvement in the visual system: implications in allergic and neurodegenerative diseases. Cytokine Growth Factor Rev. 2004 Dec;15(6):411-7. Review. PMID:15561599

Micera A, Quaranta L, Esposito G, Floriani I, Pocobelli A, Saccà SC, Riva I, Manni G, Oddone F.
Morgan TH. (1932). "The scientific basis of evolution". pp.286 Record Number:19330700518. Publisher:London Faber and Faber, Ltd.

Nakamura K, Harada C, Okumura A, Namekata K, Mitamura Y, Yoshida K, Ohno S, Yoshida H, Harada T. Effect of p75NTR on the regulation of photoreceptor apoptosis in the rd mouse. Mol Vis. 2005 Dec 29;11:1229-35. PMID:16402023

Nelson JD. Impression cytology. Cornea. 1988;7(1):71-81. PMID:3280239

Micera A, Lambiase A, Stampachiacchiere B, Sgrulletta R, Normando EM, Bonini S, Bonini S. Nerve growth factor has a modulatory role on human primary fibroblast cultures derived from vernal keratoconjunctivitis-affected conjunctiva. Mol Vis. 2007 Jun 21;13:981-7. PMID:17653039

Offit K. (2011). "Personalized medicine: new genomics, old lessons". Hum Genet. 130(1): 3–14. doi:10.1007/s00439-011-1028-3. PMCID: PMC3128266

Patel DS, Arunakirinathan M, Stuart A, Angunawela R. Allergic eye disease. BMJ. 2017 Nov 2;359:j4706. doi: 10.1136/bmj.j4706. Review. No abstract available. PMID:29097360

Pavelić K, Martinović T, Kraljević Pavelić S. (2015). "Translational and Personalized Medicine".MEDICINE, LAW & SOCIETY Vol. 8, pp. 25 – 33. doi:10.18690/8.25-33 PMID:1847878
Pritchard DE, Moeckel M, Villa MS, Housman LT, McCarty CA, McLeod HL. (2017). "Strategies for integrating personalized medicine into healthcare practice". Personalized Medicine. 14(2):141-152 doi:10.2217/pme-2016-0064

Qureshi A, Niazi JH, Kallempudi S, Gurbuz Y. Label-free capacitive biosensor for sensitive detection of multiple biomarkers using gold interdigitated capacitor

arrays. Biosens Bioelectron. 2010 Jun 15;25(10):2318-23. doi: 10.1016/j.bios.2010.03.018. Epub 2010 Mar 21. PMID:20381333

Ripandelli G, Rossi T, Scarinci F, Stirpe M. Encircling scleral buckling with inferior indentation for recurrent retinal detachment in highly myopic eyes. Retina. 2015 Mar;35(3):416-22. doi: 10.1097/IAE.0000000000000389. PMID:25360789

Rocco ML, Balzamino BO, Esposito G, Petrella C, Aloe L, Micera A. NGF/anti-VEGF combined exposure protects RCS retinal cells and photoreceptors that underwent a local worsening of inflammation. Graefes Arch Clin Exp Ophthalmol. 2017 Mar;255(3):567-574. doi: 10.1007/s00417-016-3567-8. Epub 2016 Dec 24.

Rocco ML, Balzamino BO, Petrocchi Passeri P, Micera A, Aloe L. Effect of purified murine NGF on isolated photoreceptors of a rodent developing retinitis pigmentosa. PLoS One. 2015 Apr 21;10(4):e0124810. doi: 10.1371/journal.pone.0124810. eCollection 2015. PMID:25897972

Sacchetti M, Lambiase A, Cortes M, Sgrulletta R, Bonini S, Merlo D, Bonini S. Clinical and cytological findings in limbal stem cell deficiency. Graefes Arch Clin Exp Ophthalmol. 2005 Sep;243(9):870-6. Epub 2005 Mar 19. PMID: 15778841

Schargus M, Ivanova S, Kakkassery V, Dick HB, Joachim S. Correlation of Tear Film Osmolarity and 2 Different MMP-9 Tests With Common Dry Eye Tests in a Cohort of Non-Dry Eye Patients. Cornea. 2015 Jul;34(7):739-44. doi: 10.1097/ICO.0000000000000449. PMID:25909238

Seitz B, Lisch W. Stage-related therapy of corneal dystrophies. Dev Ophthalmol. 2011;48:116-53. doi: 10.1159/000324081. Epub 2011 Apr 26. Review. PMID:21540634

Shi Z, Birman E, Saragovi HU. Neurotrophic rationale in glaucoma: a TrkA agonist, but not NGF or a p75 antagonist, protects retinal ganglion cells in vivo. Dev Neurobiol. 2007 Jun;67(7):884-94. Erratum in: Dev Neurobiol. 2007 Sep 15;67(11):1547-8. PMID:17506493

Siliprandi R, Canella R, Carmignoto G. Nerve growth factor promotes functional recovery of retinal ganglion cells after ischemia. Invest Ophthalmol Vis Sci. 1993 Nov;34(12):3232-45. PMID:8225858

Singh R, Joseph A, Umapathy T, Tint NL, Dua HS. Impression cytology of the ocular surface. Br J Ophthalmol. 2005 Dec;89(12):1655-9. Review. PMID:16299150

Skeie JM, Tsang SH, Mahajan VB. Evisceration of mouse vitreous and retina for proteomic analyses. J Vis Exp. 2011 Apr 3;(50). pii: 2795. doi: 10.3791/2795. PMID:21490583

Thiel MA, Bossart W, Bernauer W. Improved impression cytology techniques for the immunopathological diagnosis of superficial viral infections. Br J Ophthalmol. 1997 Nov;81(11):984-8. PMID:9505824
Tseng SC. Staging of conjunctival squamous metaplasia by impression cytology. Ophthalmology. 1985 Jun;92(6):728-33. PMID:3897935

Tsubota K, Fujihara T, Saito K, Takeuchi T. Conjunctival epithelium expression of HLA-DR in dry eye patients. Ophthalmologica. 1999;213(1):16-9. PMID:9838252

Ventola CL. (2014). "Medical Applications for 3D Printing: Current and Projected Uses". P T. 39(10): 704–711. PMCID: PMC4189697

Vogenberg FR, Barash CI, Pursel M. (2010). "Personalized Medicine Part 2: Ethical, Legal, and Regulatory Issues". P T. 35(11): 624-626, 628-631, 642. PMCID: PMC2993070

Vujosevic S, Micera A, Bini S, Berton M, Esposito G, Midena E. Aqueous Humor Biomarkers of Müller Cell Activation in Diabetic Eyes. Invest Ophthalmol Vis Sci. 2015 Jun;56(6):3913-8. doi: 10.1167/iovs.15-16554. PMID:26087356

Vujosevic S, Micera A, Bini S, Berton M, Esposito G, Midena E. Proteome analysis of retinal glia cells-related inflammatory cytokines in the aqueous humour of diabetic patients. Acta Ophthalmol. 2016 Feb;94(1):56-64. doi: 10.1111/aos.12812. Epub 2015 Aug 13. PMID:26268591

Wilson BJ and Nicholls SG. (2015). "The Human Genome Project, and recent advances in personalized genomics". Risk Manag Healthc Policy. 2015; 8: 9–20. doi:10.2147/RMHP.S58728. PMCID: PMC4337712

Yang Z, Huo S, Shan Y, Liu H, Xu Y, Yao K, Li X, Zhang X. STAT3 repressed USP7 expression is crucial for colon cancer development. FEBS Lett. 2012 Sep 21;586(19):3013-7. doi: 10.1016/j.febslet.2012.06.025. Epub 2012 Jun 27. PMID:22750444

Zhang L and Hong H. (2015). "Genomic Discoveries and Personalized Medicine in Neurological Diseases". Pharmaceutics. 2015 Dec; 7(4): 542–553. doi: 10.3390/pharmaceutics7040542. PMCID: PMC4695833

ACKNOWLEDGMENTS

Firstly, I would like to express my sincere gratitude to my Supervisor Prof. Loredana Zollo for the continuous support of my Ph.D. study and related research, for her patience, motivation, and immense knowledge and to my Co-Supervisor Dr. Alessandra Micera, for her insightful comments and encouragement, but also for the hard question which incented me to widen my research from various perspectives.

I thank my fellow lab mates for the stimulating discussions, for all the fun we have had in the last years. I also thank my friends in the Lab. of Biomedical Robotics and Biomicrosystems for their support in engineering doubts.

I will always thank my family: my angel mom, my dad and my brother for supporting me spiritually throughout this hard process and my life in general.

And at last, I thank my wife Graziana and my little princess, you are my life, my strength, my joy, my breath.